Brain, Behavior, and Immunity xxx (xxxx) xxx

Contents lists available at ScienceDirect

Brain Behavior and Immunity

journal homepage: www.elsevier.com/locate/ybrbi

Type I interferon mediated induction of somatostatin leads to suppression of ghrelin and appetite thereby promoting viral immunity in mice

Susanne Stutte [a,j], Janina Ruf [a], Ina Kugler [a], Hellen Ishikawa-Ankerhold [b], Andreas Parzefall [c], Peggy Marconi [d], Takahiro Maeda [e], Tsuneyasu Kaisho [f], Anne Krug [a], Bastian Popper [g], Henning Lauterbach [h], Marco Colonna [i], Ulrich von Andrian [j], Thomas Brocker [a,*]

[a] Institute for Immunology, Faculty of Medicine, LMU Munich, Germany
[b] Department of Internal Medicine I, University Hospital, LMU Munich, Germany
[c] Research Unit Analytical Pathology, Helmholtz Zentrum München, Neuherberg, Germany
[d] Department of Chemical and Pharmaceutical Sciences (DipSCF), University of Ferrara, Italy
[e] Departments of Island and Community Medicine, Nagasaki University Graduate School of Biomedical Sciences, 1-7-1, Sakamoto, Nagasaki City, Japan
[f] Department of Immunology, Institute of Advanced Medicine, Wakayama Medical University, Kimiidera 811-1, Wakayama 641-8509, Japan
[g] Biomedical Center (BMC), Core Facility Animal Models, Medical Faculty, LMU Munich, Germany
[h] Bavarian Nordic GmbH, Martinsried, Germany
[i] Washington University, School of Medicine, St. Louis, USA
[j] Department of Immunology, Blavatnik Institute, Harvard Medical School, Boston, USA

ARTICLE INFO

Keywords:
Anorexia
Type 1 interferon
Plasmacytoid dendritic cells
Ghrelin
Viral infection

ABSTRACT

Loss of appetite (anorexia) is a typical behavioral response to infectious diseases that often reduces body weight. Also, anorexia can be observed in cancer and trauma patients, causing poor quality of life and reduced prospects of positive therapeutic outcomes. Although anorexia is an acute symptom, its initiation and endocrine regulation during antiviral immune responses are poorly understood. During viral infections, plasmacytoid dendritic cells (pDCs) produce abundant type I interferon (IFN-I) to initiate first-line defense mechanisms. Here, by targeted ablation of pDCs and various *in vitro* and *in vivo* mouse models of viral infection and inflammation, we identified that IFN-I is a significant driver of somatostatin (SST). Consequently, SST suppressed the hunger hormone ghrelin that led to severe metabolic changes, anorexia, and rapid body weight loss. Furthermore, during vaccination with Modified Vaccinia Ankara virus (MVA), the SST-mediated suppression of ghrelin was critical to viral immune response, as ghrelin restrained the production of early cytokines by natural killer (NK) cells and pDCs, and impaired the clonal expansion of $CD8^+$ T cells. Thus, the hormonal modulation of ghrelin through SST and the cytokine IFN-I is fundamental for optimal antiviral immunity, which comes at the expense of calorie intake.

1. Introduction

Infections, inflammation, physical trauma and cancer cause symptomatic behavioral responses, referred to as "sickness behavior", a programmed defense response leading to symptoms including depression, lethargy, reduction in appetite (anorexia) and body weight loss (Allison and Ditor, 2014; Hart, 1988; Machida et al., 2014). "Sickness behavior" evolved to reorganize the organism's priorities for preserving bodily resources, such as maintaining the high energetic cost of fever and coping with infectious pathogens (Hart and Hart, 2018). Recently, it was shown that the consequence of anorexia depends on the type of infection (Wang et al., 2016): while anorexia-induced fasting metabolism is protective in bacterial infection (Wang et al., 2016), this nutritional state is detrimental during viral diseases (Wang et al., 2016). Some inflammatory cytokines have been shown to mediate sickness behavior (Dantzer, 2001; Kelley et al., 2003), but in the case of anorexia and food uptake, neither the exact regulation, nor the correlation to immunity during infection is well understood.

Plasmacytoid dendritic cells (pDCs) are rare innate immune cells that are marked by an expression of SiglecH, B220, PDCA-1 and Ly6C (Asselin-Paturel et al., 2001). They recognize single-stranded RNA and viral and microbial DNA and respond with a robust secretion of IFN-I

* Corresponding author at: Institute for Immunology, Biomedical Center Munich, Grosshaderner Str. 9, 82152 Planegg-Martinsried, Germany.
E-mail address: tbrocker@med.uni-muenchen.de (T. Brocker).

https://doi.org/10.1016/j.bbi.2021.04.018
Received 11 January 2021; Received in revised form 6 April 2021; Accepted 20 April 2021
Available online 23 April 2021

that is often followed by their cell death (Brown et al., 2009; Swiecki et al., 2011). This early wave of IFN-I has important general protective anti-viral effects by modulating proliferation, survival and differentiation of other immune cells (Crouse et al., 2015). Furthermore, sensing of IFN-I by endothelia and epithelia cells of the brain have recently been attributed to the psychologic and cognitive components of "sickness behavior" (Blank et al., 2016) and thereby established and important connection between immunity and the behavioral changes of sick individuals. Interestingly, therapeutically administered IFN-I in patients with malignancies, multiple sclerosis or hepatitis-C virus infection often led to severe anorexia (Capuron et al., 2002; Capuron and Miller, 2004; Leuschen et al., 2004).

Here, we observed a rapid IFN-I production by dying pDCs and identified that this IFN-I promoted the expression of the neuropeptide hormone somatostatin (SST). SST is a small peptide with a half-life of two minutes that can be released by brain neurons and by delta cells of the digestive system (Rorsman and Huising, 2018). In the brain, SST inhibits the release of the growth hormone (Burgus et al., 1973), whereas, in the pancreas, it regulates the release of glucagon and insulin to maintain a blood glucose homeostasis (Hauge-Evans et al., 2009). We identified that IFN-I promotes a rise of SST in the blood, which suppresses the hunger hormone ghrelin and reduces appetite, leading to rapid weight loss. Blocking the receptor of IFN-I (IFN-R) or SST signaling rescued ghrelin suppression and prevented anorexia. In accordance with this, the injection of recombinant IFN-I led to an upregulation of SST and to an inhibition of ghrelin which was followed by a loss of appetite. Furthermore, during viral immunization, we could show, that the suppression of ghrelin is mandatory, since ghrelin inhibited the production of innate inflammatory cytokines, shown here for IFN-α by pDCs and IFN-γ by NK cells, that subsequently led to low numbers of anti-viral $CD8^+$ T effector cells. Our results demonstrated that pDC-ablation leads to release of IFN-I and that this early cytokine controls the balance between early immunity and calorie intake via the SST and ghrelin pathway, opening up novel possibilities to treat sickness-induced anorexia and to modulate the outcome of immunity.

2. Materials and methods

2.1. Animals

C57BL/6J and BDCA2-DTR (Tg(CLEC4C-HBEGF)956Cln/J, pDC-DTR), OT1 CD45.1 (Tg(TcraTcrb)1100Mjb/J)xPtprc^a) mice and IFNAR-KO (IFN-ar1tm1Agt/Mmjax) mice were obtained from Jackson Laboratories, XCR1-venus-DTR were a kind gift from T. Kaisho (Yamazaki et al., 2013). All mice are on C57BL/6NJ background and backcrossed for at least 6 generations. Mice were bred in the animal facilities of the LMU, Harvard Medical School, Boston, or University of Ferrara, Italy. Mice were studied at 6–8 weeks of age and were sex matched. Animal experiments were performed in accordance with the guidelines of the local Ethical Committees, as well as in accordance with NIH guidelines, approved by the IACUC and COMS of Harvard Medical School, government of Bavaria and the ethical committee (0/30/17, 02/17/194), University of Ferrara, Italy. The animals in the animal husbandries were kept in a low-pathogen environment to protect them from infections. Each room is inspected every six months (standard and extended program alternately) using litter sentinel animals according to the FELASA program to detect possible infections. Cages: IVC system, type II, 370 cm^2 (Integra-Biosciences, Fernwald, Germany) with cage trays made of light-reducing amber polysulfone. Stocking density: maximum 4 adult animals. Access regulation: person-limited access control. Light regime: 12-hour rhythm; light dimmed during the day. Bedding: autoclaved bedding granules (Lignocell, Rettenmeier, Rosenberg). Feed, husbandry: mouse husbandry extrudate, V1536 Feed. Breeding: mouse breeding extrudate, V1126 (Ssniff Special Diets, Soest). Water: tap water in autoclaved bottles. Enrichment: The nesting material Sizzlenest (Ssniff Special Diets, Soest) is provided in sufficient quantities to build a complete shelter in each cage. Also, cardboard tubes are offered as shelters (Play tunnel, Bioscape, Castrop-Rauxel). Room climate: temperature 22–24 °C, relative humidity 50 ± 5%.

2.2. Ablation of pDCs

For pDC ablation an initial dose of 150 μg anti-mouse CD317 (PDCA-1) antibody (clone 927, Biolegend) followed by daily injections of 50 μg for the following days were administered intraperitoneally (i.p.) as indicated for 4 or 6 days. Mice received i.p. injections of DT (8 ng/g; Calbiochem-Merck), administered through insulin syringes. Mice that received treatment were randomly assigned to cages so that each cage contained both mice with experimental and control treatment (PBS or DT or WT and pDC-DTR mice – both treated with DT).

2.3. CSS-application

Cyclo-somatostatin (CSS) (Tocris) was applied if not indicated otherwise with 10 μg/mouse i.p. in PBS twice a day. For short term treatment ghrelin (Tocris) was applied with 20 μg/mouse i.p. every 2 h for 6 h.

2.4. Ghrelin supplementation

If not stated otherwise, ghrelin was supplied in drinking water with 3 μg/ml that was daily exchanged. The water consumption was controlled by measuring the weight of water before and after treatment and compared to control animals that received tap water with the solvent (dest. water). The average consumption of water was 3.5–5 ml per day/mouse which was measured by weighing the bottles. This means a mouse had taken up 10.5–15 μg of ghrelin/day orally. We confirmed the gained results, by treating mice with ghrelin by i.p. injections that were applied twice daily (20 μg/mouse) for 5–7 days.

2.5. IFN-I blocking

Blocking of IFN-I signal was performed by application of IFN-R-blocking antibody (clone MAR1-5A3, Biolegend). Treatment started 1 day before DT injection and was continued by applying 250 μg/mouse i.p. daily or every other day. Isotype control (clone MOPC21, Biolegend) was given accordingly.

2.6. CD4 T cell depletion

CD4 T cells were depleted via application of LEAF-purified anti-CD4 antibody (GK1.5, Biolegend) (first injection: 150 μg followed by daily 40 μg). FACS staining on day 5 controlled the success of depletion.

2.7. Treatment with IFN-α

Mice were injected once with recombinant universal IFN-α (PBL Assay Science) (5000U/ mouse i.v.). 4 h later serum was harvested to measure induction of SST and ghrelin repression. To evaluate the impact on appetite IFN-α was injected in the evening and food consumption was measured the following morning (16 h later).

2.8. TLR-ligands, virus and CSS

R848 (100 μg, Invivogen), HSV-1 (KOS) (10^7 pfu) or MVA (5×10^7 TCID) were injected iv. 30 mg/kg Poly(I:C) (invivogen) were applied i.p. as published previously (Wang et al., 2016). Mice were sacrificed after 6 h and blood was harvested via heart puncture. Food consumption after R848, Poly(I:C), MVA, and HSV was measured after 6 h. For blockade of SST CSS (0.4 μg/g, Tocris) was applied by i.p. injection.

2.9. pDC and NK cell responses

Mice were injected with MVA (5×10^7 TCID) i.v. and every 2 h with CSS (10 μg/mouse) or ghrelin (20 μg/mouse) i.p. The spleen was harvested and cell suspension was incubated for 4 h with Brefeldin A (10 μg/mL; Sigma-Aldrich) in supplemented RPMI media (RPMI-1670 GlutaMAXTM-I (GIBCO) with supplements (10% FCS (GIBCO), 1% P/S (GIBCO), 1% NEAA (GE-Healthcare), 0.05 mM ß-MeEtOH (GIBCO)). Cell surface and intracellular epitopes were then stained with flow cytometry antibodies.

2.10. T cell response

For measuring the $CD8^+$ T cell response mice were injected i.v. with 0.5×10^6 OT1 $CD45.1^+$ $CD8^+$ T cells and 24 h later with 5×10^7 TCID MVA-OVA (MVA-mBNbc126). A group of mice were additionally treated with ghrelin in drinking water for 7 days (exchanged every other day). After 7 days the spleen was harvested and endogenous and transferred T cells were analyzed for OVA and MVA specific T cells responses. For that splenic cell suspension was re-stimulated for 1 h either with PBS or 1 μg/ml of OVA- or MVA specific peptide (OVA257-267 or B8R (TSYKFESV) together with CD107a-PE, followed by 3 h incubation in the presence of Brefeldin A (10 μg/mL; Sigma-Aldrich). Cells were surface-stained for 30 min at 4 °C. Intracellular staining for IFN-γ was performed using a Cytofix/Cytoperm Kit (BD Biosciences) according to the manufacturer's protocol.

2.11. Tissue processing

Blood was harvested via heart puncture and transferred into 2 mM EDTA/PBS. Red blood cells were lyzed with Pharm Lyse ™ (BD) and cell pellet were resuspended in FACS buffer (2 mM EDTA/PBS, 1% FCS). BM was flushed from femur with FACS buffer (1% FBS, 0.5 mM EDTA in PBS) and red cells were lysed with Pharm Lyse ™ (BD). Spleens were digested with Collagenase 4 (250 μg/ml) and DNase 1 (400 μg/ml) for 20 min at 37 °C and strained through a 100 μm nylon mesh and washed in 0.5 mM EDTA/PBS. Red cell lysis followed (Pharm Lyse ™, BD). The single-cell suspension was washed with FACS buffer, resuspended for 15 min at 4 °C in Fc-Block and then stained with appropriate antibodies (identified below). Counting beads (Thermo Fisher) were added for calculating absolute cell numbers of acquired samples/tissue when measured by FACS Canto (BD) or cells were counted by Casy cell counter (OLS Omni Life Sciences). For histology of visceral epididymal adipose tissue (VAT) organs were placed into 4% PFA and further processed for paraffin embedding. Pancreatic tissue was weighted and lysed in Tissue Extraction Reagent I (Thermo Fisher) with protease inhibitor (Roche). After centrifuging to remove debris, solution was frozen at −80 °C until further measurements.

2.12. Flow cytometry and antibodies

FACS buffer (1% BSA, 0.5 mM EDTA/PBS) was used for staining cells. Samples were pre-incubated with Fc-Block (TruStain fcX™ (anti-mouse CD16/32) antibody, Biolegend, 1:100) for 15 min 4 °C before being stained at 4 °C with specific antibodies. Dead cells were excluded with a live/dead gate by using zombie aqua (Biolegend). Antibodies conjugated to different fluorochromes and specific for the following molecules were as follows (if not indicated otherwise - used 1:200 and ordered from Biolegend): SiglecH (551, 1:300), B220 (RA3-6B2), Ly6C (BD, AL-21, 1:400), PDCA-1 (927, 1:300), CD45 (30-F11), CD19 (6D5), CD11b (M1/70, 1:500), TCRβ (G572597), CD3 (145-2C11), CD11c (N418), Ly6G (1A8), F4/80 (BM8), NK1.1 (CD161c, PK136) and XCR1 (ZET). Tbet (4B10), IFN-γ (XMG1.2, 1:400) and human IFN-α (Miltenyi, 1:100) were stained intracellularly with BD Fixation/Permeabilization Solution Kit. Cell doublets were excluded by comparison of side-scatter width to forward-scatter area. Counting beads (Thermo Fisher, eBioscience) were added for calculating absolute cell numbers of acquired samples. Staining of phosphorylated proteins was performed after staining for surface epitopes conjugated to FITC or Alexa 647 and Alexa 405. Cells were fixed with 1.5% PFA for 15 min followed with methanol fixation at −20 °C for at least 30 min. Cells were washed twice in PBS and stained intracellularly by using Perm buffer III (BD, Heidelberg) and p-IRF7 (Ser437/438 cell signaling, 1:100) or p-Akt (Ser473, cell signaling, 1:100) and goat anti-rabbit Alexa 488 or anti-rabbit-Cy5 (Thermo Fisher, 1:300). Ghrelin receptor staining was performed by using GHS-R (GHSR) antibody (abcam, ab95250, 1:100 in PBS) for 30 min on ice, and after extensive washing secondary antibody goat anti-rabbit Alexa 488 (1:400) was used. As isotype control rabbit isotype antibody (Thermo Fisher was used).

Flow cytometry samples were acquired with FACSCantoII from BD Biosciences. Samples were analyzed using FlowJo-software.

2.13. Image flow cytometry

Cells were stained by surface markers via FACS antibodies with 2% formaldehyde in PBS for 20 min at 4 °C, and permeabilized in PBS containing 0.1% Triton X-100 and 1% BSA, cells were stained with purified IRF7 (1:100, EPR4718, abcam or PA5-79519 Thermo Fisher) antibody for 30 min at 4 °C followed by a second antibody staining using goat-anti rabbit FITC (Biolegend) or anti-rabbit Alexa 488 (1:300, Thermo Fisher). Finally, the cells were stained with DRAQ5 (ebioscience) and measured with the AMNIS ImageStream (Millipore). 5000 pDCs were at least acquired. Similarity score between IRF7 and DRAQ5 was calculated using the IDEAS software similarity feature. Frequency of cells with IRF7 translocation was calculated.

2.14. ELISA

Blood samples were taken by heart puncture and serum was isolated after clogging for 1 h at RT. Total ghrelin EIA were obtained from Sigma-Aldrich (Germany) and performed according to the manufacturer's protocol with detection limit of 161 pg/ml. SST-competitive ELISA (sst-14 and sst-28) was obtained from Cloud-Clone Corp, USA (sensitivity: 2.77 pg/ml). Insulin was measured by Insulin ELISA according to the protocol (Mercodia Sweden, sensitivity $\leq$ 0.2 ng/ml). C-Peptide was quantified by EIA (Sigma Aldrich, sensitivity 772 pg/ml). Emission was analyzed by an ELISA reader (promega). Murine IFN-α was measured from serum and supernatants according to the manufacturer's protocol (Verikine–HS mouse IFN-α- all subtype ELISA kit (PBL), sensitivity: 2.38 pg/ml). Legendplex analyses (anti-viral response panel) of serum samples were performed according to the manufacturer's protocol (Biolegend) and analyzed on Cytoflex S (Beckman Coulter).

2.15. In vitro culture

Murine bones were flushed and red cells of the bone marrow (BM) were lysed (Pharmlys, BD) and taken into culture for 7 days with recombinant (100 ng/ml) FLT3L (Biolegend) in RPMI-1640 GlutaMAXTM-I (GIBCO) with supplements (10% FCS (GIBCO), 1 mM sodium pyruvate (GIBCO), 1% P/S (GIBCO), 1% NEAA (GE-Healthcare), 0.05 mM ß-MeEtOH (GIBCO)). Cells were harvested by flushing petri dishes with cold PBS. Purity of pDCs was between 65 and 75% as determined by FACS. For culture purposes 5×10^6 pDC/ml were incubated in 96 round-bottom wells. For treating cells in-vitro with DT we incubated cells in RPMI1640 supplemented with 1% BSA and 10 μg/ml DT.

The human pDC cell line CAL-1 (Maeda et al., 2005) was incubated in 1% BSA/RPMI1640, 1 mM sodium pyruvate (GIBCO), 1% P/S (GIBCO), 1% NEAA (GE-Healthcare), 0.05 mM ß-MeEtOH (GIBCO) in 48 well plate with 3×10^6 cells/ml. 7 h later cells were harvested and stained for AMNIS analysis with IRF7. To measure IFN-α production, cells were incubated with media (RPMI1640, 1% BSA), DT (10 μg/ml) for 8 h. Brefeldin 1 μg/ml was added for the last 4 h. Cells were stained

for viability dye and universal IFN-α–PE (Miltenyi) and measured by flow cytometry.

2.16. mRNA detection

Tissues (whole stomach, total spleen, total pancreas) were each homogenized in 1 ml trizol (QIAzol Lysis reagent). Total brain and 0.5 g of liver were homogenized in 3 ml trizol. After spinning down the debris the supernatant (1 ml) was used to isolate the RNA. After the addition of 200 µl chloroform and centrifugation the aqueous phase was transferred into a new tube and mixed with 70% ethanol. The mix was further transferred to RNeasy mini spin columns of the RNeasy mini kit (Qiagen, Hilden, Germany) and RNA was isolated according to the manufactur's protocol. 1 µg of total RNA was transcribed into cDNA with the iScript kit (Biorad, California, USA). The qPCR was performed with Sybr® Green (Biorad) and the primers were designed with the Roche probe library. The House-keeping gene 18S was chosen as this ribosomal RNA is highly expressed across tissues, cells, and experimental treatments. It does not change with activation of cells and remains stable through treatments (Bas et al., 2004). qPCR was performed with Biorad thermo cycler (T100). The following primers were used to identify 18S mRNA and SST-mRNA: SST: F: agagaatgatgccctggagc; R: gggagagggatcagaggtct and 18S F: gcaattattccccatgaacg, R: gggacttaatcaacgcaagc. Relative expression was calculated to non-treated cells/ WT-mice, which were set to 1.

2.17. Metabolic studies and measurement of food intake

Body weight and food intake were monitored daily by weighing body and chow. After sacrificing, the heart and the muscle (m. rectus femoris) of one femur and the whole epididymal adipose fat pads (visceral adipose tissue; VAT) were weighed. Fasting the mice for a period of 5–6 h in the morning, allowed to measure fasting blood glucose levels by taking a drop of blood from the tail vain to be analyzed with OneTouch Ultra mini test stripes (LifeScan Inc., Wayne, USA). For insulin measurements mice were fasted for 5 h, 1 g/kg glucose was applied orally and 30 min later blood was drawn.

The food was weighted manually daily by taking the food out of the feeding rack to a scale. Only big pieces were given back to the rack to prevent falling down of little pieces through the grid. When little pieces were seen on the floor their weight was taken into account of the measurement. We did not observe any abnormal chewing or spilling of food. Daily monitoring allowed tight control of behavioral changes.

2.18. Statistical analyses

The statistical tests used included unpaired Student's *t*-test and two-way ANOVA tests. P values of ≤ 0.05 were considered significant, * = $P < 0.5$; ** = $P < 0.01$; *** = $P < 0.001$. No exclusions of data points or mice were performed. Pilot studies were used for estimation of the sample size required to ensure adequate power. GraphPad Prism software 7 and 8 were used.

3. Results

3.1. Depletion of pDCs caused weight loss

We investigated the physiological consequences of pDC-death and ablated pDCs for consecutive days by injecting diphtheria toxin (DT) in transgenic mice expressing the receptor of diphtheria toxin (DTR) under a pDC specific promoter (Swiecki et al., 2010). As reported before (Swiecki et al., 2010), the injection of DT caused a transient removal of pDCs from the bone marrow (BM), that were reconstituted within 48 h (Supplementary Fig. 1A). However, this pDC-depletion modality spared substantial numbers of immature SiglecH^{+}CD317^{-} and even some mature SiglecH^{+}CD317^{+} pDCs in the BM (Supplementary Fig. 1B). We improved the ablation efficacy in BM and spleen by injecting DT every 24 h (Supplementary Fig. 1A, Supplementary Fig. 2A–D). The remaining cells of the 24 h DT treatment were SiglecH^{+}B220^{low} (Supplementary Fig. 2C, D), that had been described to be immature pDCs and pre-DC progenitors with pDC-differentiation capability (Schlitzer et al., 2015). Interestingly, using a pDC-depleting monoclonal antibody (mAb) anti-CD317 (Blasius et al., 2006) was far less efficient, removing only 40–50% of all pDCs in BM. By applying a daily DT treatment, we ensured a prolonged pDC-absence for 6 days (Supplementary Fig. 2B).

Unexpectedly, and in contrast to all other pDC-depletion treatments, the most efficient removal of pDCs caused strong physiological alterations, as mice lost approximately 15–20% of their body weight within these 6 days (Fig. 1A, Supplementary Fig. 2E). This was accompanied by a loss of 25–35% of muscle mass as shown for skeletal (*m. rectus femoris*; Fig. 1B, left) and heart muscle (Fig. 1B, right). Furthermore, the 80% weight reduction of the visceral adipose tissue (VAT) (Fig. 1C) went along with a contraction of adipocytes (Fig. 1D, E), indicating strong catabolism of adipocyte energy stores. Therefore, the pDC-ablation phenotype resembled weight loss and muscle atrophy seen during various diseases (cachexia). In addition, the metabolic disturbance caused by pDC-ablation was also manifested by a strong drop in fasting blood glucose levels (Fig. 1F). However, as soon as the pDC-depletion was stopped, the induced weight loss was completely reversed and mice acquired normal weight again within 4–5 days (Fig. 1G). Taken together, the removal of pDCs led to rapid, but reversible changes in body weight and metabolism of mice.

3.2. pDC depletion results in anorexia by increased level of SST

To understand if weight loss was caused by reduced calorie input, the appetite of mice was monitored by measuring their food consumption over time. Beginning at day 3 of pDC-depletion, the appetite was significantly reduced which further decreased over time of pDC-depletion (Fig. 2A). The decrease in food consumption was reversible, as rapidly upon stopping the DT-treatment, mice regained appetite (Fig. 2B). One major regulator of appetite is the hormone ghrelin (Nakazato et al., 2001). When the stomach is empty and contracted ghrelin is released by stomach wall delta-cells (Howick et al., 2017) to signal to the brain to increase food consumption (Cowley et al., 2003; Zigman et al., 2006). Interestingly, within 4 days of pDC-depletion, ghrelin levels in serum were significantly lowered compared to control mice (Fig. 2C), although the stomachs of pDC-depleted mice were empty, contracted and without substantial nutritional content (Fig. 2D). One negative regulator of ghrelin release is SST, which is, in addition to other sources, co-expressed in the stomach (Shimada et al., 2003). Already by day 3 of pDC-ablation, we found the SST serum levels significantly increased (Fig. 2E). To identify the source for increased SST expression, we performed qPCR analysis of the major SST-producing organs. Interestingly, after the continuous ablation of pDCs, the brain and pancreas showed no significant changes in SST gene expression, while the stomach underwent a 5-fold SST upregulation (Fig. 2F). In addition to the regulation of ghrelin, SST is also a key regulator of insulin to control blood glucose levels (Hauge-Evans et al., 2015). Indeed, insulin was low in serum and could not be induced in pDC-ablated mice (Fig. 2G). Also, the C-peptide, which is co-released with insulin, showed a similar reduction (Fig. 2H). In contrast, insulin accumulated in pancreatic tissue, suggesting that insulin release, rather than production itself, was suppressed (Fig. 2I), a typical effect of SST (Strowski et al., 2000).

To understand if the rise in SST-levels were directly responsible for weight loss upon pDC-depletion, we blocked SST signaling by applying its antagonist cyclosomatostatin (CSS). CSS application during pDC-depletion completely rescued weight loss and food consumption, while it did not alter these parameters in wild type control mice (Fig. 2J). Furthermore, the serum levels of ghrelin were rescued in pDC ablated mice in presence of CSS (Fig. 2K). Accordingly, when mice were

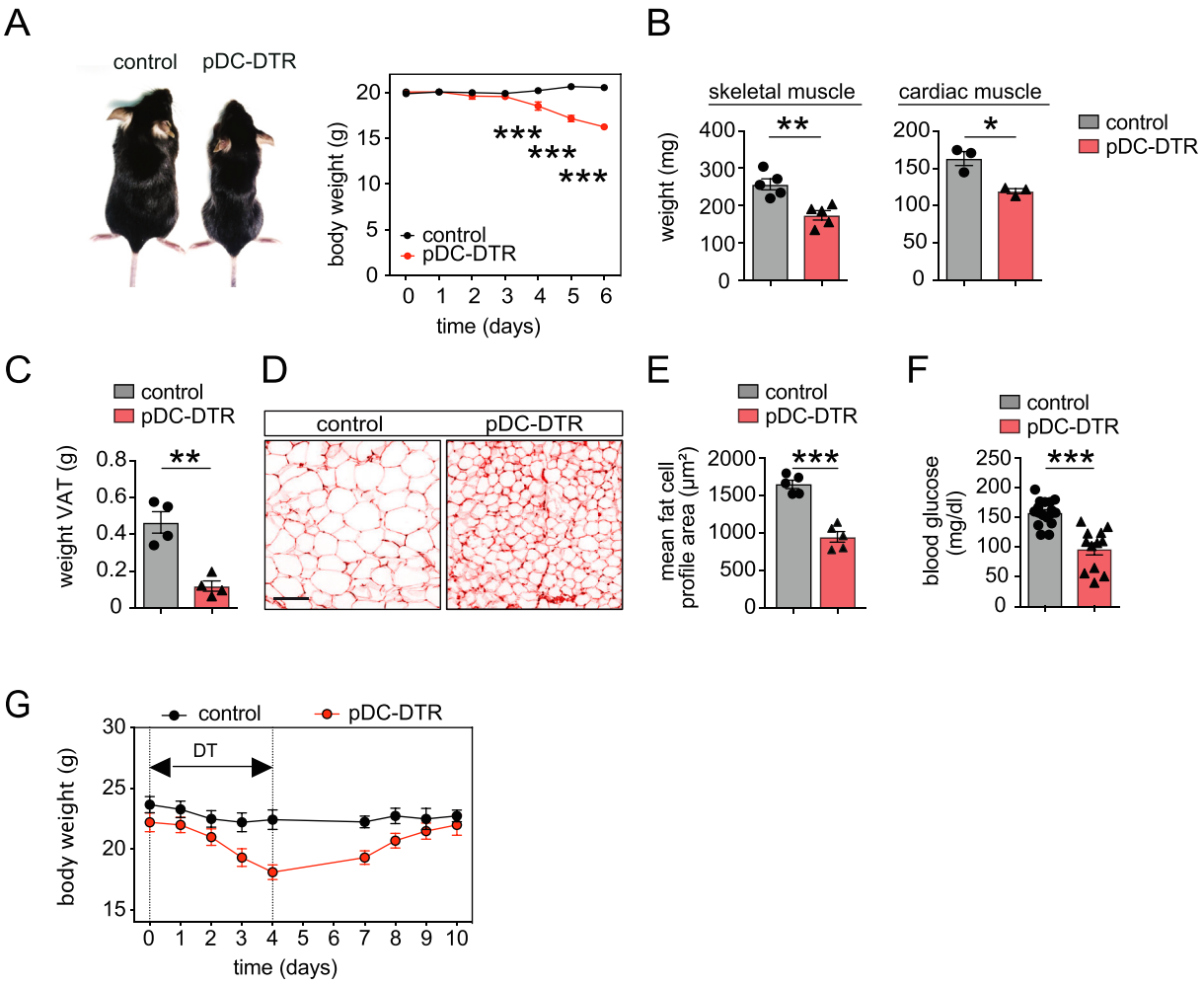

Fig. 1. Depletion of pDC results in metabolic changes. (A) WT and pDC-DTR mice were treated with DT for 5 days and body phenotype was photographed on day 5 of DT-treatment (left panel) and weight loss of mice (control: black, pDC-DTR: red) was monitored over time (right panel) with n = 8–24 of animals per time point. (B) Weight of skeletal muscle (*m. rectus femoris*) and cardiac muscle were determined on day 5 of pDC depletion and compared to WT control mice. (C) Weight of epididymal visceral adipose tissue (VAT) was determined on day 5 of DT-treatment. (D) Histological paraffin sections from VAT (H&E staining, size bar represents 100 µm) were generated and (E) the mean area of adipocytes within each section were measured. Each dot represents mean counted value of sections of one mouse. (F) Mice were fasted for 5 h on day 5 of pDC-depletion and blood glucose levels were measured. (G) WT and pDC-DTR mice were treated with DT. After the last DT injection on day 4, mice were given time to recover. Body weight of mice was measured at indicated time points. Shown data are representative of two (D, E, G, (n = 5)) or three (A-C, F, (n = 3–24)) independent experiments, and were analyzed by two-way unpaired Student's *t*-test (B, C, E, F). Data from (A) was analyzed by two-way ANOVA test. Data are shown as arithmetic means and error bars (A-G) denote SEM * $P < 0.05$; **$P < 0.01$; *** $P < 0.001$. (For interpretation of the references to colour in this figure legend, the reader is referred to the web version of this article.)

supplemented during pDC-depletion with exogenous ghrelin, the weight loss and food consumption were partly rescued (Fig. 2L).

We next investigated whether the SST upregulation and ghrelin downregulation are general mechanisms, that can be similarly observed in other pDC ablation models. To this end we depleted pDCs in wild type mice with a daily anti-CD317 mAb treatment. Although this method was less efficient for the removal of pDCs, when compared to pDC-depletion obtained by DT-injection in pDC-DTR mice (Supplementary Fig. 2B), it was also accompanied by moderate weight loss (Supplementary Fig. 2E). In a kinetic study, anti-CD317-depleted wild type mice showed approximately 10% weight loss on the fifth day of antibody treatment (Supplementary Fig. 3A). This was accompanied by a moderate trend of SST upregulation, which was, however, not statistically significant (Supplementary Fig. 3B). Interestingly, a significant downregulation of both ghrelin and C-peptide could be observed (Supplementary Fig. 3B). This data suggests that both models of pDC ablation, either with a pDC specific antibody or by DT in pDC-DTR mice, lead to suppression of ghrelin and loss of appetite, decreased food uptake and reduction in body weight.

3.3. pDC-ablation phenotype is mediated by IFN-I

To understand the positive regulation of SST we tested whether the observed effects were pDC-specific. To this end, we deleted other immune cell types by various methods. Although the deletion of CD4 T cells by injecting anti-CD4 antibody was highly efficient (Supplementary Fig. 4A), we could hardly observe any weight loss in treated mice (Fig. 3A). In addition, DT-mediated ablation of the XCR1$^+$ DC-subset in XCR1-DTR mice (Supplementary Fig. 3B), using a 3 times higher dose of DT as compared to pDC-DTR mice, induced only a slight weight reduction of 10% the initial weight (Fig. 3A). In contrast, the removal of pDCs resulted in 20% weight loss (Fig. 3A). These results suggested that the observed effects did not depend on the relative amounts of dead cells, as for example CD4 T cell depletion causes far greater dead cell numbers than the depletion of rare pDCs. We concluded that the pDC ablation phenotype has been mediated by pDC-specific properties. As the physiological changes were mediated by induced cell death of pDCs, serum was analyzed for inflammatory cytokines associated with cell death (Cowley et al., 2003). Indeed, the depletion of pDCs led to a more

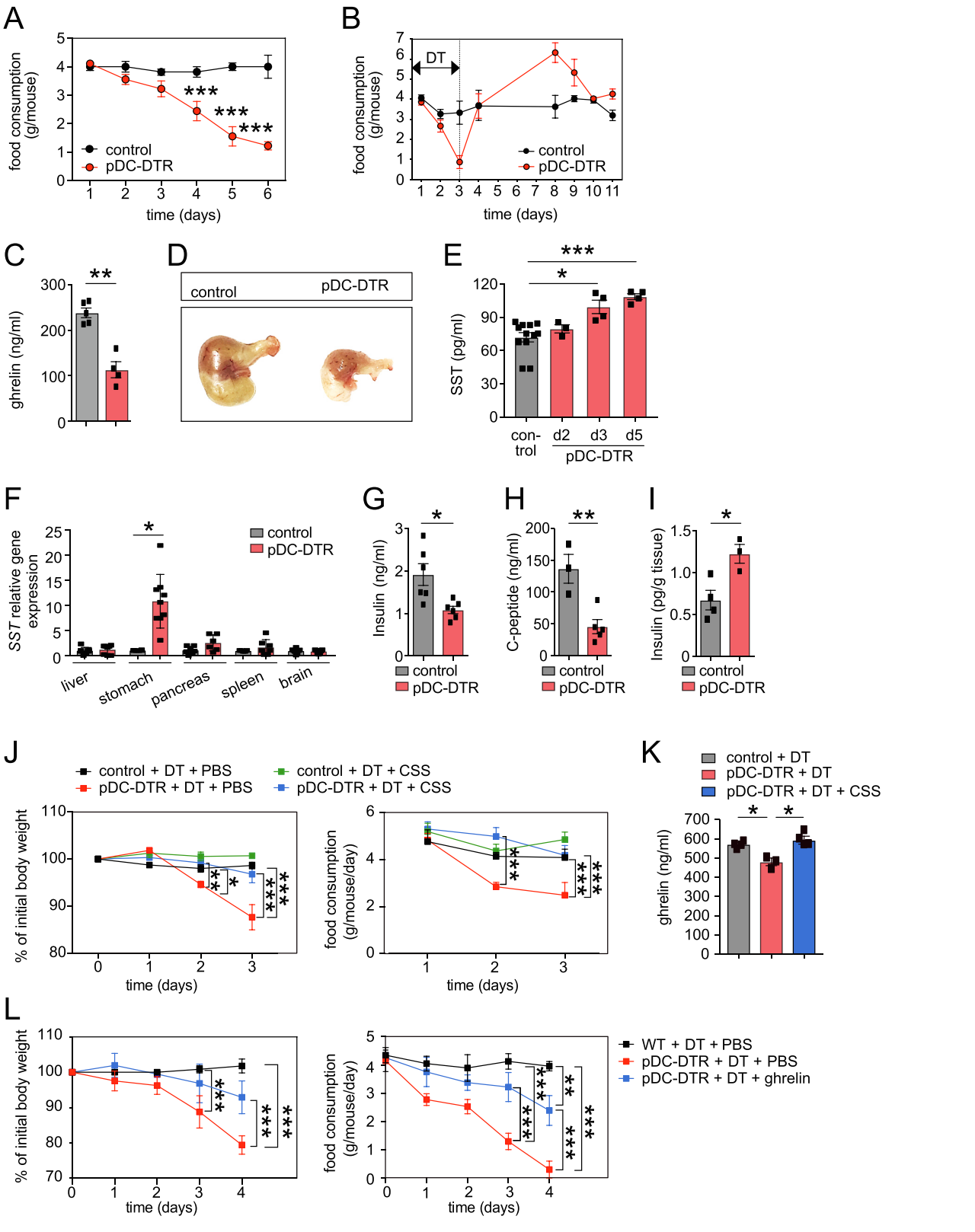

(caption on next page)

Fig. 2. pDC-depletion results in decrease of ghrelin due to increased SST levels. (A) Control (black) and pDC-DTR mice (red) received DT for 6 days and food consumption was measured daily. (B) Control (black) and pDC-DTR mice (red) received DT daily until day 3 and mice recovered until day 11. Food consumption during this time frame was monitored. (C) At day 5 of DT injection serum was drawn from WT and pDC-DTR mice. Total ghrelin was measured by ELISA. (D) Pictures of stomachs were taken on day 5 of DT injection of WT and pDC-DTR mice. (E) Serum SST-levels were measured by ELISA from WT (grey bar) and pDC-DTR mice (red bar) at indicated time points of DT treatment. (F) SST-producing organs such as liver, stomach, pancreas, spleen and brain were homogenized in Trizol ® after organs have been harvested from WT control (grey bars) or pDC-DTR (red bars) mice treated with DT for 5 days. SST mRNA levels were quantified by real-time qPCR and relative gene expression was calculated by setting the mean of control organs as 1. Individual expression of control or pDC-DTR organs were calculated. (G) WT and pDC-DTR mice were treated for 5 days with DT and after fasting for 5 h 1 g/kg glucose was applied orally and serum levels of insulin and (H) C-peptide were determined by ELISA. Insulin content from pancreatic tissue was determined and correlated to tissue weight (I). (J) WT (black), pDC-DTR mice (red) were treated daily with DT and one group of WT (green), and pDC-DTR (blue) mice received additionally 2x daily cyclosomatostatin (CSS). Body weight and food uptake were tracked over time. (K) WT (grey), pDC-DTR mice (red) were treated daily with DT and one group of pDC-DTR mice (blue) received additionally 2x daily cyclosomatostatin (CSS, blue). Serum was analyzed for ghrelin by ELISA. (L) WT (black) and pDC-DTR (red) mice were treated with DT plus PBS and pDC-DTR (blue line) mice were treated with DT plus ghrelin and body weight and food consumption were monitored. All experiments were repeated twice with 4–6 animals per group (n = 4–6) and similar outcome. Statistics were performed with Student's *t*-test (C, E-I, K) or two-way repeated measures ANOVA test (A, J, L). Error bars show SEM * $P < 0.05$; ** $P < 0.01$; *** $P < 0.001$. (For interpretation of the references to colour in this figure legend, the reader is referred to the web version of this article.)

than 5-fold increase of IFN-ß, IL-17a, and IL-6 (Fig. 3B). Furthermore, IL-1ß, MCP-1, TNFα, and IL-27 rose 2-fold, while IL-10 was decreased (Fig. 3B). Interestingly, blocking of IL-6 or IL-1ß signaling with monoclonal antibodies during pDC depletion had no impact on weight reduction (Supplemental Fig. 4D and E). In contrast, the sole blockade of IFN-I-receptor (IFN-R) signaling during DT-induced pDC ablation prevented weight loss (Fig. 3C, blue line) in comparison to pDC-DTR mice that received the isotype control antibody (Fig. 3C, red line). Similarly, the removal of pDCs in pDC-DTR-mice that were deficient for the IFN-R (IFNAR-ko × pDC-DTR) showed no reduction in body weight (Fig. 3D, blue line), confirming a central role of IFN-I in mediating anorexia and cachexia following pDC depletion.

Furthermore, the levels of SST, ghrelin and C-peptide remained unchanged in presence of IFN-R blockade (Fig. 3E), indicating a direct regulatory link between IFN-I and hormonal mediators. To directly prove the link between IFN-I and the endocrine system we applied recombinant universal IFN-α to wild type mice. Strikingly, IFN-α directly boosted systemic SST levels and lowered ghrelin levels (Fig. 3F) that resulted in a reduction of the appetite by half when compared to control mice (Fig. 3F). This demonstrates, that the early cytokine IFN-I mediated the anorexic effects observed during pDC ablation and that IFN-α is capable to stir the functions of the endocrine system. IFN-I thereby performs as a negative regulator of the feeding behavior.

3.4. pDCs produced IFN-I before DT-mediated cell death

pDC-depleted mice had significantly increased IFN-α serum levels already one day of DT-treatment (Fig. 4A). To test if pDCs themselves were the source of IFN-I upon DT-treatment, pDCs from pDC-DTR-mice or WT mice were exposed to DT (Fig. 4B). In contrast to control pDCs, pDCs from pDC-DTR mice produced significant amounts of IFN-α (Fig. 4B). Additionally, DT-induced cell death did not occur within the first 7 h, but rather after 18 h of DT addition (Supplementary Fig. 5A), leaving enough time for pDCs to produce IFN-I. Furthermore, *de novo* IFN-α production is initiated by IRF7 which is constitutively present in the cytoplasm of pDCs. Upon cell activation IRF7 gets phosphorylated and translocated to the nucleus where it initiates the IFN-I gene transcription (Honda et al., 2005; Marie et al., 2000). We observed by imaging flow cytometry that PBS-treated pDCs from both, WT control mice as well as pDC-DTR mice have IRF7 located in the cytoplasm (Fig. 4C). However, upon DT-treatment, pDC-DTR pDCs revealed shuttling of IRF7 to the nucleus, while WT pDCs did not alter their IRF7 nuclear content (Fig. 4C). Normally, murine cells are insensitive to DT and only the transgene expression of primate DTR (HB-EGF) in pDC-DTR mice allowed the depletion of pDCs by DT (Saito et al., 2001). In contrast, all human cells are naturally DT-sensitive due to a constitutive and ubiquitous DTR expression. Therefore, we incubated cells of the human pDC-cell line CAL1 (Maeda et al., 2005) with DT and found that this similarly initiated the translocation of IRF7 to the nucleus (Fig. 4D). Furthermore, DT-treatment induced significant IFN-α expression in human pDCs (Fig. 4E) as shown by intracellular cytokine staining, supporting the finding that pDCs were one source of IFN-I production before DT-mediated cell death.

3.5. Ghrelin suppressed $CD8^+$ T cell immunity during viral infection

In numerous viral infections, IFN-I is produced early and rapidly (Supplementary Fig. 6A) (McNab et al., 2015) to activate, modulate and amplify the innate and adaptive immunity. To test if these infections are accompanied by an upregulation of SST, mice were treated with R848, a synthetic TLR7-ligand, which mainly targets pDCs to induce IFN-α-production *in vivo* (Asselin-Paturel et al., 2005; Kawai and Akira, 2011). The R848 injection mediated an increase of SST serum levels and a strong decrease of food consumption (Fig. 5A, B). Also, poly (I:C), a synthetic TLR3 ligand raised the SST levels and stopped food consumption in mice (Fig. 5A, B). Similarly, immunizing mice with Modified Vaccinia Virus Ankara (MVA), a very potent vector for vaccination against infectious diseases and cancer, known to induce IFN-I production (Dai et al., 2014), raised systemic levels of SST and rapidly mediated a stop of food consumption (Fig. 5A, B). Also, herpes simplex virus (HSV (KOS)), which induces IFN-α in an IRF7-dependent fashion (Honda et al., 2005) and causes transient weight loss in C57BL/6 mice (Reading et al., 2006), showed significantly elevated SST levels and again, decreased the food consumption in infected mice (Fig. 5A, B). We concluded that viral infection and TLR-mediated inflammation increased SST, that consequently resulted in suppression of appetite. It was still unclear why early during infection SST is enhanced and loss of appetite induced. To identify if SST during viral immunization is beneficial for the initiation of an efficient anti-viral immune response, we used the MVA vaccine, that is a robust vector suitable for addressing a wide variety of infectious diseases and cancers. It is approved to vaccinate against smallpox (JYNNEOS ®) and Ebola (MVA-BN® FILO) and currently in clinical trials to vaccinate against several forms of cancer (Bavarian Nordic, Denmark). To test if there is a necessity for the suppression of ghrelin to succeed in immunity, we immunized mice with an MVA-vector that additionally encoded the model antigen ovalbumin (OVA). 7 days after the immunization and the adoptive transfer of OVA-specific TCR-transgenic OT1 $CD8^+$ T cells, the T cell response was analyzed. Splenic endogenous $CD8^+$ T cells (data not shown) and OT1 $CD8^+$ T cells were both expanding with and without ghrelin supplementation (Fig. 5C). While the frequencies of $CD8^+$ T cells were comparable with or without ghrelin, the total cell numbers were strongly reduced in mice supplemented with ghrelin (Fig. 5C, right panel). In non-immunized control mice (PBS), the addition of ghrelin did not interfere with the numbers of OT1 T cells nor of endogenous $CD8^+$ T cells (Fig. 5C). This suggested that ghrelin exerts negative effects only during active immune responses. Furthermore, in MVA-OVA vaccinated mice, the addition of ghrelin did not alter the activated phenotype of $CD8^+$ T cells ($CD62L^{low}CD44^{high}$) when compared to mice that received PBS only (Supplementary Fig. 6B). Interestingly, upon re-stimulation

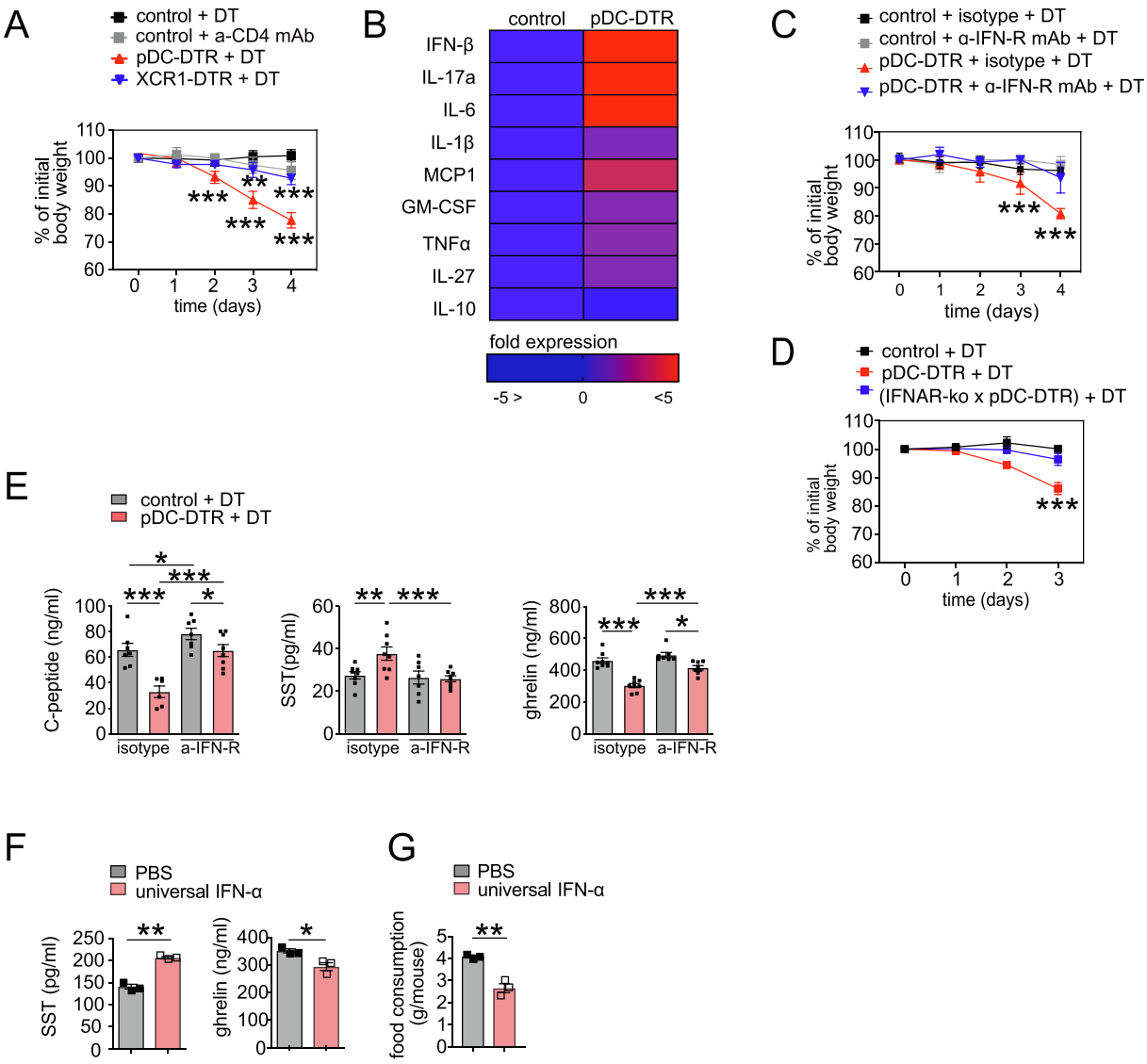

Fig. 3. pDC-ablation phenotype is mediated by IFN-I. (A) Body weight of DT induced depletion of pDCs in pDC-DTR mice (red line) was compared to DT-treated control mice (WT, black line) and other mouse models of ablated immune cells. To deplete XCR1$^+$ DCs (blue line), mice were injected with DT according to the protocol (Yamazaki et al., 2013) and injection of monoclonal antibody against CD4 was used to deplete CD4$^+$ T cells (grey line). Body weight was tracked daily over 5 days. (B) WT and pDC-DTR mice were treated with DT for 5 days and serum was analyzed for inflammatory cytokine expression by Legend plex analysis. Levels were calculated as fold level of mean WT and plotted as heat map. (C) WT (control) and pDC-DTR mice were injected daily with DT and blocking antibody to IFN-R (MAR1- 5A3) or isotype control (isotype, MOPC-21). Body weight was tracked over time and compared to initial body weight that was set to 100. (D) WT mice (control), pDC-DTR and IFNAR-ko × pDC-DTR mice were daily injected with DT. Body weight was tracked over time and compared to initial body weight that was set to 100%. (E) Control and pDC-DTR mice were injected daily with DT and blocking antibody to IFN-R (MAR1- 5A3) or isotype control (isotype, MOPC-21). Serum from mice was harvested at day 4 and ELISA for C-peptide, SST and ghrelin were performed. The data combined two independent experiments with n = 3–5 mice per group. (F) WT mice were injected with PBS (grey bar) or rec. IFN-α (i.v.) (red bar) and 4 h later blood was harvested. Analyses of serum by ELISA for SST and ghrelin were performed. (G) Food uptake was measured 18 h after PBS or rec. INF-α injection. Data is representative of two independent experiments with (n = 3) mice per group and was analyzed by two-way-ANOVA (A, C, D, E) or unpaired Student's *t*-test (F-G). Data are shown as arithmetic means and error bars (A-L) denote SEM * P < 0.05; ** P < 0.01; *** P < 0.001. (For interpretation of the references to colour in this figure legend, the reader is referred to the web version of this article.)

with the OVA peptide, we found that OT1 T cells were significantly reduced in IFN-γ expressing cells when ghrelin had been supplemented for 7 days (Fig. 5D). This corresponded to the general reduction of T cell numbers (Fig. 5C). In conclusion, the data suggested that the presence of ghrelin during viral immune responses suppressed the development of antigen specific CD8$^+$ T cells. Therefore, to obtain optimal expansion of anti-viral CD8$^+$ T cells, the inhibition of ghrelin is absolutely required.

3.6. The IFN-I-SST-ghrelin-pathway controlled early innate immune cell signaling during viral infection and inflammation

The clonal expansion of antigen-specific CD8$^+$ T cells depends on the priming milieu within secondary lymphoid organs (Dixit et al., 2004). Therefore, MVA vaccination was employed together with PBS, recombinant ghrelin or CSS (Fig. 6A). After 6 h, PBS and MVA co-administration showed increased levels of IFN-α (Fig. 6B, MVA + PBS). In contrast, the *in vivo* blockade of SST by CSS (Fig. 6B, MVA + CSS) as well as the administration of exogenous ghrelin (Fig. 6B, MVA + ghrelin) decreased the serum levels of IFN-α at least by half (Fig. 6B), indicating a negative impact of CSS or ghrelin on this early cytokine. Much of the early IFN-I during MVA inflammation is provided by pDCs (Waibler et al., 2007). Interestingly, the exogenous administration of ghrelin during MVA immunization led to a lower number of pDCs with phosphorylated IRF7 (p-IRF7) (Fig. 6C) and lower levels of p-IRF7

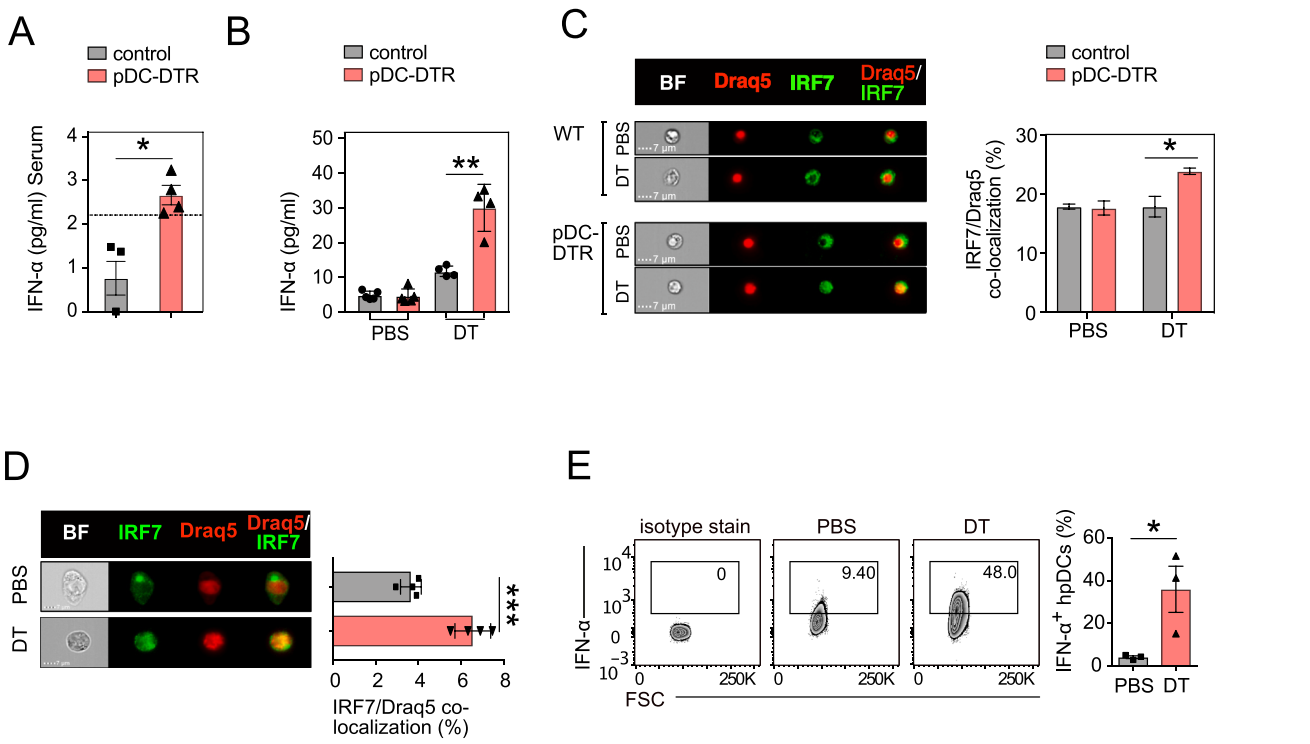

Fig. 4. DT treatment of pDCs induces IRF7 translocation and IFN-α release. (A) Serum of control (WT, grey bar) and pDC-DTR (red bar) mice was harvested one day after DT treatment and analyzed for IFN-α. Dotted line indicates the limit of detection of this assay. (B) WT control and pDC-DTR BM-derived pDCs were incubated for 18 h *in vitro* with DT or PBS. Supernatant was harvested and analyzed for IFN-α. (C) BM-derived pDCs from control (WT) and pDC-DTR mice were incubated with DT or with PBS in media for 7 h and stained for B220 and CD11b. Cells were intracellularly stained for IRF7 (green) and Draq5 (red, nucleus) and analyzed by AMNIS imaging flow cytometry. AMNIS data of colocalization of IRF7 and Draq5 in $B220^{+}$ $CD11b^{-}$ cells was analyzed with *Ideas* software. (D) CAL1 cells were incubated with DT and harvested after 7 h. Cells were intracellularly stained for IRF7 and Draq5 and analyzed by AMNIS imaging flow cytometry. (E) CAL1 cells were incubated with DT for 8 h and the last 4 h Brefeldin A was additionally added. Cells were harvested and stained for human IFN-α. The data are representative of two (A-E) independent experiments (n = 3–5) and were analyzed by unpaired Student's *t*-test (A-E). Error bars denote SEM *P < 0.05; **P < 0.01; ***P < 0.001. (For interpretation of the references to colour in this figure legend, the reader is referred to the web version of this article.)

(Fig. 6C, MFI right) when compared to PBS controls. As phosphorylation of IRF7 is essential for its translocation to the nucleus to initiate IFN-I expression, ghrelin directly limited the capacity of pDCs to produce IFN-I (Fig. 6C).

Furthermore, the major cytokine IFN-γ is produced by natural killer (NK) cells early during immune responses (Farsakoglu et al., 2019; Martin-Fontecha et al., 2004) and directly acts on $CD8^{+}$ T cells and controls their numbers during clonal expansion (Whitmire et al., 2005). Here, after 6 h, MVA and PBS co-administration led to high levels of IFN-γ (Fig. 6D, MVA + PBS), while the *in vivo* blockade of SST by CSS (Fig. 6D, MVA + CSS) or exogenous ghrelin (Fig. 6D, MVA + ghrelin) lowered serum IFN-γ levels at least by two thirds (Fig. 6D). The activation of lymphocytes is generally initiated by Akt-phosphorylation (Henson et al., 2009) and a defective Akt-phosphorylation has been previously correlated with impaired NK cell functions (Wang et al., 2013). Indeed, we found that treating with CSS and ghrelin during MVA-vaccination significantly reduced the phosphorylation of Akt at Ser473 in NK cells, when compared to mice that received MVA with PBS only (Fig. 6E). Moreover, while MVA-immunization resulted in strong IFN-γ protein expression in NK cells (Fig. 6D), the presence of the SST-inhibitor CSS or exogenous ghrelin strongly reduced the proportion of $IFN\text{-}\gamma^{+}$ NK cells (Fig. 6D). Mechanistically, it has been shown that the capacity to produce IFN-γ by NK cells positively correlated with the expression of the transcription factor T-bet, while a downregulated T-bet causes NK cell dysfunction (Gill et al., 2012). During MVA vaccination, both exogenous ghrelin and CSS significantly reduced intracellular levels of T-bet in NK-cells (Supplementary Fig. 7A). This argued for a diminished functional status of NK cells when either the natural upregulation of SST or the repression of ghrelin is counteracted during vaccination. Interestingly, compared to PBS + MVA, the treatment with ghrelin or CSS had no impact on NK cells and their early activation phenotype, as all groups had a comparable surface expression of CD69 (Supplementary Fig. 7B). In summary, this data indicated that the presence of ghrelin or the blockade of SST signaling impaired the function of pDCs and NK cells. Furthermore, the regulation of SST by IFN-I was a prerequisite for optimal pDC and NK cell functions as it inhibited the presence of ghrelin and with that provided an effective priming environment.

3.7. Ghrelin receptor was expressed by innate immune cells

Ghrelin reduced the activation of key transcription factors in pDCs and NK cells leading to lowered levels of IFN-α and -γ. To investigate if ghrelin exerts these effects directly on innate immune cells, we analyzed if pDCs and NK cells express the ghrelin receptor (growth hormone secretagogue receptor or ghrelin receptor (GHSR)). Approximately 15–20% of all pDCs (Fig. 7A) and 10% of all NK cells (Fig. 7B) expressed GHSR in a steady state. The administration of MVA increased $GHSR^{+}$ pDCs up to 25–30% (Fig. 6A), that went along with an induction the activation marker CD69 (Fig. 7A, middle). Similarly, MVA also induced GHSR expression by NK cells, while matured $CD11b^{+}$ NK cells showed a higher GHSR expression upon MVA immunization (Fig. 7B). We concluded that activated pDCs and NK cells increased their surface GHSR expression, to potentially allow a negative feedback loop to control their secretory functions.

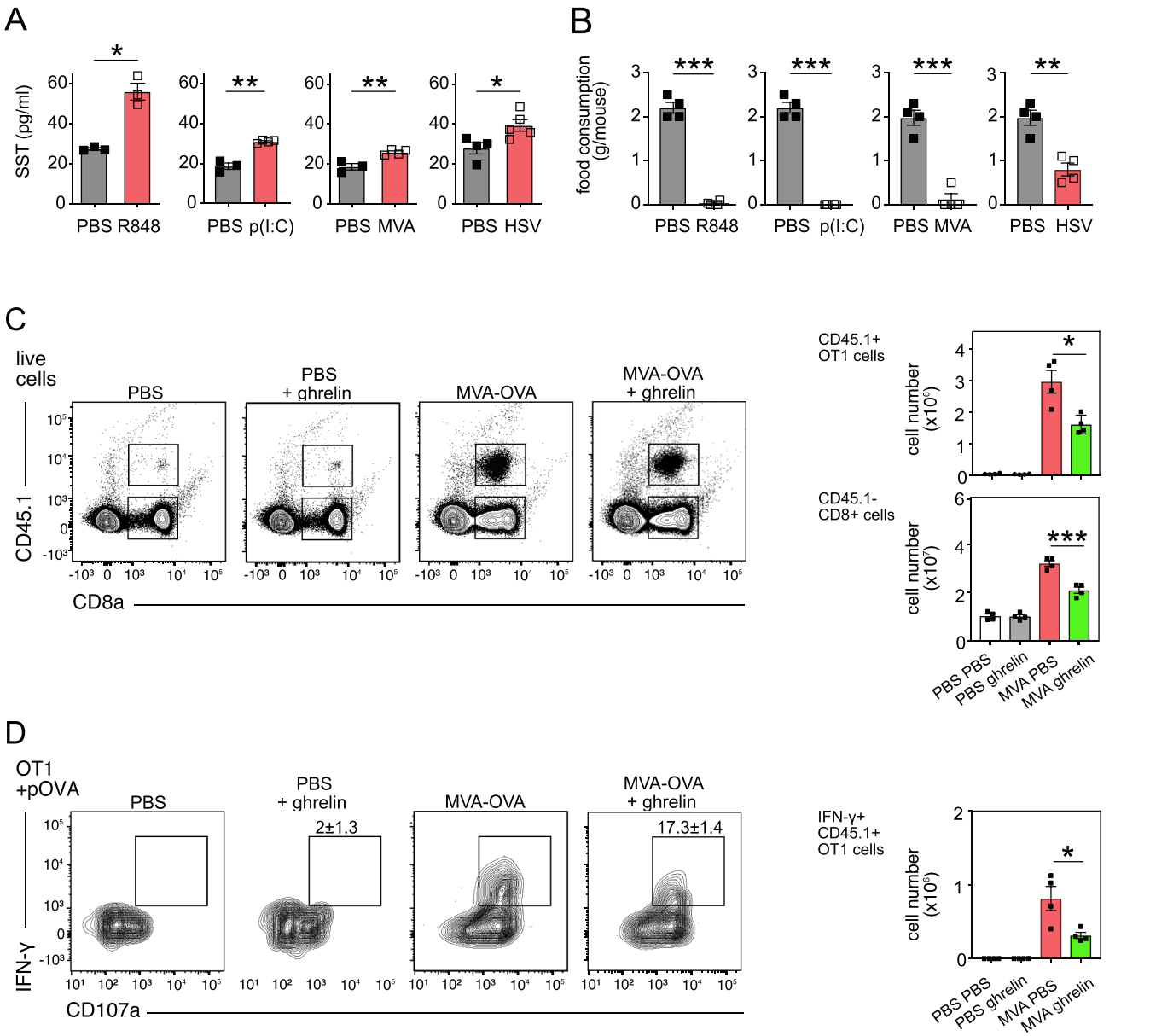

Fig. 5. SST and ghrelin regulation are required during immune responses *in vivo*. Mice were injected with PBS (grey bar) or R848 (100 μg), poly(I:C) (30 mg/kg), 5×10^7 TCID modified vaccinia virus Ankara (MVA) or 5×10^6 pfu HSV-1(KOS) i.v. (red bar) and 6–8 h later serum was isolated and analyzed for SST by ELISA (A) and the food consumption was measured (B). (C-D) CD45.1$^-$ C57BL/6 mice were adoptively transferred with 5×10^5 CD45.1$^+$ OT1 T cells and immunized 24 h later i.v. with MVA-OVA (5×10^7 TCID) or injected with PBS instead. Two groups of mice received additionally recombinant ghrelin in drinking water, which was continuously renewed for 7 days. (C) Frequencies of CD8$^+$CD45.1$^+$ OT1 T cells and endogenous CD8$^+$CD45.1$^-$ T cells were determined from spleen cell suspensions by flow cytometry on day 7 post immunization. Numbers indicate frequencies of the respective populations in the gate. Total cell numbers are shown in bar graphs. (D) T cells were restimulated *in vitro* with OVA peptide (pOVA, SIINFEKL) and IFN-γ was stained intracellularly on CD8$^+$CD45.1$^+$ OT1 T cells by flow cytometry. Numbers on the gates represent percentages of IFN-γ$^+$ cells. Bar graphs show absolute numbers of IFN-γ$^+$ OT1 T cells per spleen. The data are representative of two independent experiments (n = 3–5) and were analyzed by unpaired Student's *t*-test. Error bars denote SEM; *P < 0.05; **P < 0.01; *** P < 0.001. (For interpretation of the references to colour in this figure legend, the reader is referred to the web version of this article.)

4. Conclusion

Viral and bacterial infections are associated with behavioral characteristics, such loss of appetite (anorexia). Prolonged anorexia results in drastic weight loss that represents a leading cause of morbidity and mortality. Understanding the mechanism causing anorexia has remained elusive. Here, we demonstrate how viral infections induce anorexia and why this in an evolved strategy to induce potent anti-viral immune responses.

The early IFN-I, mainly produced by plasmacytoid dendritic cells, upregulates the hormone somatostatin in the stomach that in turn suppresses the hunger hormone ghrelin and thereby mediates loss of appetite. Interestingly, this pathway is essential for the optimal induction of anti-viral immunity as NK cells and pDCs fail to provide a milieu for efficient T cell priming in presence of ghrelin. In summary, we showed a direct crosstalk of IFN-I with hormones expressed within the stomach to regulate early viral immunity on the cost of appetite.

5. Discussion

IFN-I has initially been recognized to interfere with viral replication (Isaacs and Lindenmann, 1957; Isaacs et al., 1957) and to activate the

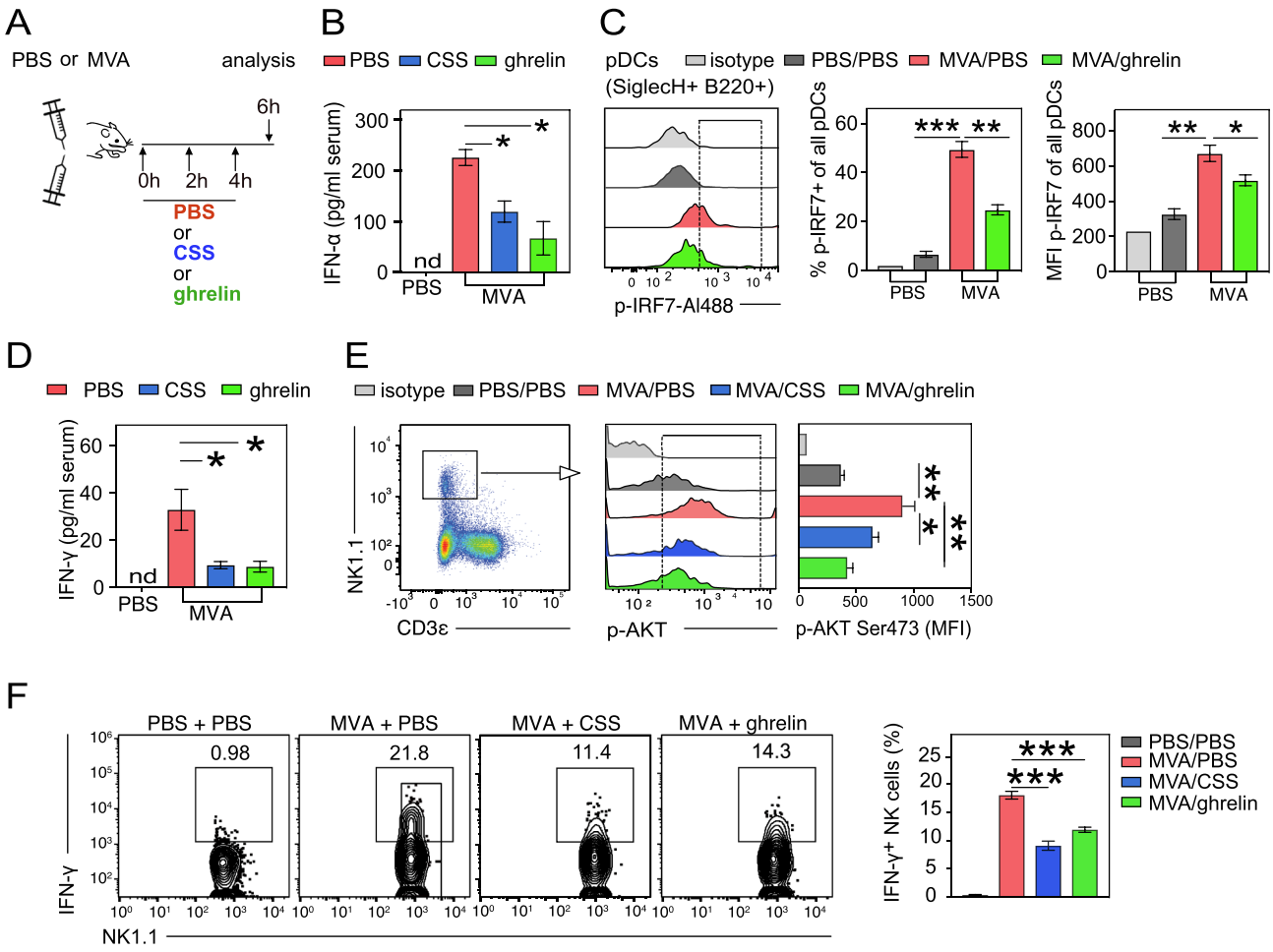

Fig. 6. The IFN-1/SST/ghrelin-axis controls early innate immune mechanisms during infection and inflammation. (A) Mice were immunized with PBS only or MVA with either additionally PBS (red), CSS i.p. (blue) or ghrelin i.p. (green) every 2 h. 8 h post immunization serum was collected for determination of IFN-α (B). (C) Mice were treated for 6 or 8 h with PBS (dark grey bar) or MVA and every 2 h PBS (red bar) or recombinant ghrelin (green bar) was applied. Splenic pDCs were stained intracellularly for phosphorylated IRF7 (p-IRF7) or isotype control (light grey). Frequency and MFI of p-IRF7 in pDCs were calculated. (D) Mice were immunized with PBS (grey) or MVA and received either additionally PBS (red), CSS i.p. (blue) or ghrelin i.p. (green) every 2 h. 8 h post immunization serum was collected for determination of IFN-γ by Legendplex bead array (Biolegend). (E) Mice were treated as in *C* and an intracellular staining of splenic NK1.1^{+}CD3ε^{-} NK cells for p-Akt (Ser473) was performed and the MFI calculated in comparison to isotype control (light grey). (F) Mice were immunized with PBS as control (grey bar) or MVA with either additionally PBS (red bar), CSS i.p. (blue bar) or ghrelin i.p. (green bar) every 2 h. After 8 h post immunization spleens were harvested. To quantify the IFN-γ production of NK cells by intracellular flow cytometry the splenic cell suspension was re-incubated with 10 μg/ml Brefeldin-A for 4 h. IFN-γ^{+} NK cells were quantified as indicated by the gates in the individual contour plots. Numbers in gates show frequency of IFN-γ^{+} NK cells in the respective analyses. The data are representative of two (B, D, n = 3–5) or three (C-E, F, n = 3–5) independent experiments and were analyzed by unpaired Student's *t*-test (B-F). Error bars denote SEM * $P < 0.05$; ** $P < 0.01$; *** $P < 0.001$. (For interpretation of the references to colour in this figure legend, the reader is referred to the web version of this article.)

immune system (Wang and Fish, 2012). In some cases, it is also deleterious due to toxic effects or by mediating inflammatory or autoimmune syndromes (Pascual et al., 2010; Tomasello et al., 2014). IFN-I can be expressed by many cell types, but upon viral stimulation pDCs secrete very rapidly high amounts of IFN-I as they uniquely, constitutively express the transcription factor IRF7 (Gilliet et al., 2008; Tomasello et al., 2018). We found that the exposure of DT-sensitive pDCs to DT caused translocation of IRF7 to the nucleus and initiated IFN-α expression. For researchers, the transgenic expression of high-affinity simian DTR in specific murine cells (Saito et al., 2001), is a valuable and prevalent research tool to investigate the function of these cells. Interestingly, different transgenic mouse strains expressing the DTR require individual DT doses and defined application intervals. Here, we optimized the ablation modalities for pDCs in a well-established mouse model of DTR-expression (Swiecki et al., 2010). We identified that exposure of pDCs to DT caused cell-death only after a latent period, during which pDCs survived normally, corroborating early reports on DT mediated processes (Strauss and Hendee, 1959). Although DT induces ADP-ribosylation of elongation factor-2 (Narayanan et al., 2005) resulting in toxin-modified ribosomes to stop protein synthesis, cell-entry of DT is not associated with an immediate block of RNA (Strauss, 1960) and protein synthesis (Falnes et al., 2000). Interestingly, while pDCs initiated an IFN-I response during ablation, depletion models for other immune cells were spared by this. As neither the ablation of XCR1 + conventional dendritic cells by DT nor of CD4 + T cells by antibodies induced such a strong metabolic phenotype, we excluded that general cell stress or presence of cell death was sufficient to trigger adequate signals for IFN-I release in these systems. Low levels of IFN-α induced by pDC-ablation resulted in SST-mRNA upregulation in the stomach, but not in other major places of SST production such as the pancreas or brain. The immediate target of IFN-I was demonstrated by blocking the IFN-R-signaling during pDC-ablation, which prevented the upregulation of SST. Furthermore, applying recombinant IFN-α directly augmented SST levels in blood. Interestingly, while other substances, mainly

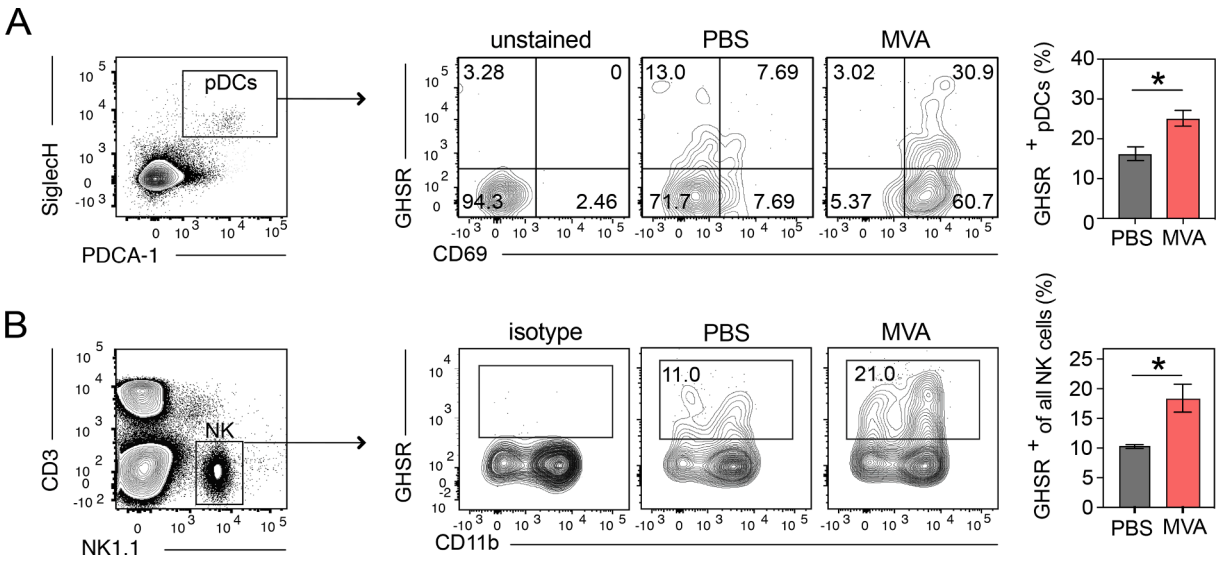

Fig. 7. Ghrelin receptor expression induced by MVA. Mice were treated with PBS (grey bar) or MVA (red bar) and 6 h later splenic pDCs (live zombie$^-$, single cells+, B220$^+$PDCA-1$^+$) (A) and NK cells (live zombie$^-$, single cells$^+$, CD3$^-$, NK1.1$^+$) (B) were analyzed for ghrelin receptor (GHSR) expression on their surface by flow cytometry. Frequency of GHSR expression was calculated. The data are representative of three independent experiments (n = 3 animals per group) and were analyzed by unpaired Student's *t*-test. Error bars denote SEM * $P < 0.05$; ** $P < 0.01$; *** $P < 0.001$. (For interpretation of the references to colour in this figure legend, the reader is referred to the web version of this article.)

neurotransmitters (Goto et al., 1981), peptide hormones (Chiba et al., 1980; Eissele et al., 1990) and metabolites (Wasada et al., 1980) have previously been shown to regulate the release of SST, a role for IFN-I on SST regulation has not been described so far. Moreover, it has been demonstrated that during *Helicobacter pylori* infection in mice, that the type-II interferon IFN-γ promoted SST expression in the stomach and thereby mediated a reduction of ghrelin (Strickertsson et al., 2011). Although the production of IFN-γ has been associated with rapid weight loss (Matthys et al., 1991) we did not find evidence for increased levels of IFN-γ after pDC ablation (data not shown). It has been reported that SST inhibits numerous physiological functions and hormones. While acting as a classical endocrine it balances glucose homeostasis in the blood by adjusting the release of insulin and glucagon (Alberti et al., 1973). Correlating with that function, we found reduced levels of insulin in serum of pDC-ablated mice, while it accumulated in the pancreas.

In addition, SST has recently been shown to negatively interfere with autoimmune immune responses, as the application of SST was suppressive in experimental autoimmune encephalomyelitis and chronic arthritis (Brod and Hood, 2011; Matucci-Cerinic et al., 1995). In contrast, here, during an anti-viral immune response, we observed a rather beneficial influence of SST. The immunization with MVA increased the systemic level of SST, which was required to inhibit ghrelin and crucial for establishing a milieu for sustained T cell expansion. When SST was blocked or ghrelin administered upon MVA-immunization, CD8$^+$ T cells failed to accumulate properly. In NK cells, the presence of ghrelin or CSS led to a failure of efficient IFN-γ expression. Strikingly, the signaling of Akt was impaired and the constitutive T-bet level reduced, indicating of an interference of ghrelin on key cellular molecules involved in regulating NK cell functions (Caraux et al., 2006; Jiang et al., 2000; Muller-Durovic et al., 2016; Wang et al., 2013). MVA vaccination together with ghrelin administration diminished the phosphorylation of IRF-7 in pDCs to one quarter. It is known, that released IFN-I triggers a positive feedback-loop in pDCs to promote their IFN-I production even further. In accordance with this, activated pDCs exhibited an increased expression of the receptor for ghrelin (GHSR) and the presence of ghrelin might have interfered or blocked this positive feedback response, resulting in an inhibition of IFN-I expression. Therefore, while optimal clonal expansion of CD8$^+$ T cells requires the presence of the cytokines IFN-I (Brewitz et al., 2017; Kolumam et al., 2005) and IFN-γ (Whitmire et al., 2005) we concluded that the presence of ghrelin is suppressive on early immune responses, making the GHSR-signaling pathway an interesting target for solving overshooting immune responses. The described signaling loop also suggests that during periods of acute ghrelin upregulation (i.e., acute hunger), mice may be more susceptible to viral infection, and vaccine administration may be suboptimal due to ghrelin's inhibitory effects on pDCs and NK cells.

Furthermore, delta cells in the stomach secrete SST, once the stomach is expanded with food content to inhibit further release of ghrelin to interrupt the feeling of hunger in the brain (DiGruccio et al., 2016; Rorsman and Huising, 2018; Shimada et al., 2003). On the opposite, mice deficient for SST display increased levels of ghrelin in the stomach (Luque et al., 2006). The administration of recombinant ghrelin enhances food intake (Nakazato et al., 2001; Tang-Christensen et al., 2004; Wren et al., 2000) and can even lead to adiposity (Tschop et al., 2000), proving a central role for ghrelin in regulating the hunger perception. Here, despite empty stomachs, pDC-DTR mice failed to release ghrelin into the circulation, due to rise in SST which consequently led to a loss of appetite. Another major hormone mediating satiety is leptin that is secreted by adipocytes. It has been reported that the concentration of serum leptin correlates with fat mass and is higher in obese and lower in lean individuals (Considine et al., 1996). As pDC-DTR mice lose weight and fat mass after pDC ablation we speculate that there is a reduction in systemic leptin levels but the impact of pDC-presence on leptin levels and the sensitivity of the leptin receptor needs to be further addressed in the future.

Extended fasting results in low blood sugar (hypoglycemia), which we also observed during pDC-depletion. Here, we identified how prolonged fasting is promoted by early IFN-I. Anorexia-induced fasting metabolism is protective in bacterial infection, but it is detrimental during viral diseases (Wang et al., 2016). Bacteria-infected mice exhibited decreased appetite and forced feeding was lethal (Murray and Murray, 1979; Wing and Young, 1980). The fasted state of anorexia was protective due to a shift from glucose to ketone bodies and free fatty acid utilization (Budd et al., 2007) thereby limiting reactive oxygen species (Wang et al., 2016). In contrast, blockade of glucose utilization was uniformly lethal in poly(I:C) and viral sepsis, as glucose was necessary to prevent the initiation of apoptosis (Wang et al., 2016). In general,

inflammatory cytokines orchestrate immune responses and affect the central nervous system by regulating food intake, energy homeostasis and sickness behavior (Dantzer, 2001; Kelley et al., 2003). Pro-inflammatory cytokines such as IL-6, IL-1β and TNFα inhibit appetite (Kent et al., 1996; Langhans and Hrupka, 1999; Mishra et al., 2019) by promoting the expression of the satiety hormone leptin (Medina et al., 1999; Turrin et al., 2004; Wueest and Konrad, 2018). IL-6 displays pleiotropic effects as it is cachectogenic and anorexigenic during acute inflammation (Timper et al., 2017; Wallenius et al., 2002; Wueest and Konrad, 2018), while it contributes to obesity when chronically expressed by adipocytes (Han et al., 2020). In contrast, chronic exposure to IL-1 and TNFα leads to tolerating the anorectic effect and a restoration of regular food intake (Mrosovsky et al., 1989; Porter et al., 1998). Indeed, while pDC ablation increased IL-6, IL-1β, and TNFα, we did not observe weight loss improvement when blocking IL-6 or IL-1β signaling. Here, only the blockade of IFN-R signaling could prevent anorexia.

The role of SST in mediating symptoms that are correlated with "sickness behavior" such as loss of appetite while promoting the anti-viral immune response is novel. This is of potential clinical relevance, as several SST analogs are already in clinical use for other indications (Borna et al., 2017; Flogstad et al., 1997). The use of SST analogs on food intake is beneficial in obesity (Tzotzas et al., 2008) and is approved to treat acromegaly and carcinoid syndrome (Riechelmann et al., 2017; Yang and Keating, 2010).

Eventually, a combination therapy of IFN-I and SST inhibitors would allow for prolonged IFN-I therapy for patients who otherwise may develop anorexia as adverse side-effect. However, more work is necessary, as it is currently not known whether the IFN-I-SST-axis also controls appetite and immunity in humans. It has been reported that the application of the SST analog octreotide suppressed insulin, stabilized weight and body mass index in obese pediatric patients (Lustig et al., 2003), and that one side effect of the SST-analogue lanreotide is weight loss. However, it is not known whether the IFN-I-SST-ghrelin cascade similarly influences human immunity. Modulation of SST function by antagonists may allow clinical interventions against anorexia seen in inflammatory diseases, cancer, and viral infections, however at the cost of full immune responses. In contrast, supplementation with ghrelin or SST antagonists might help to dampen early immune responses and to stabilize anorexia.

Author contributions

S.St. and T.B. designed the study, analyzed the data and wrote the paper. S.St., J.R. and I.K. performed experiments; A.P. performed histopathology, P.M. performed animal experiments, U.v.A. was involved in study design, M.C., A.K., H.L. and T.K. provided mice and reagents. H. I-A. performed immunohistology. B.P. performed animal experiments. All authors discussed the results and commented on the manuscript.

Declaration of Competing Interest

The authors declare that they have no known competing financial interests or personal relationships that could have appeared to influence the work reported in this paper.

Acknowledgements

We thank V. Heissmeyer for critical discussions and reading of the manuscript. We acknowledge the Core Facility Flow Cytometry at the Biomedical Center, LMU Munich, for providing FACS and AMNIS equipment.

Funding

This work was supported by Deutsche Forschungsgemeinschaft grants SFB1054 TPB03 to T.B.; SFB914 TPA06 to S.St. and T.B; SFB914 TPZ01 to H.I-A, STU 528/1-1 to S.St.; Friedrich Baur-Stiftung to S.St.

Competing Interests statement

H. Lauterbach was an employee of Bavarian Nordic GmbH. The MVA used for this study was MVA-BN®, which is Bavarian Nordic's proprietary and patented technology.

Appendix A. Supplementary data

Supplementary data to this article can be found online at https://doi.org/10.1016/j.bbi.2021.04.018.

References

Alberti, K.G., Christensen, N.J., Christensen, S.E., Hansen, A.P., Iversen, J., Lundbaek, K., Seyer-Hansen, K., Orskov, H., 1973. Inhibition of insulin secretion by somatostatin. Lancet (London, England) 2, 1299–1301.

Allison, D.J., Ditor, D.S., 2014. The common inflammatory etiology of depression and cognitive impairment: a therapeutic target. J. Neuroinflammation 11, 151.

Asselin-Paturel, C., Boonstra, A., Dalod, M., Durand, I., Yessaad, N., Dezutter-Dambuyant, C., Vicari, A., O'Garra, A., Biron, C., Briere, F., Trinchieri, G., 2001. Mouse type I IFN-producing cells are immature APCs with plasmacytoid morphology. Nat. Immunol. 2, 1144–1150.

Asselin-Paturel, C., Brizard, G., Chemin, K., Boonstra, A., O'Garra, A., Vicari, A., Trinchieri, G., 2005. Type I interferon dependence of plasmacytoid dendritic cell activation and migration. J. Exp. Med. 201, 1157–1167.

Bas, A., Forsberg, G., Hammarstrom, S., Hammarstrom, M.L., 2004. Utility of the housekeeping genes 18S rRNA, beta-actin and glyceraldehyde-3-phosphate-dehydrogenase for normalization in real-time quantitative reverse transcriptase-polymerase chain reaction analysis of gene expression in human T lymphocytes. Scand. J. Immunol. 59, 566–573.

Blank, T., Detje, C.N., Spiess, A., Hagemeyer, N., Brendecke, S.M., Wolfart, J., Staszewski, O., Zoller, T., Papageorgiou, I., Schneider, J., Paricio-Montesinos, R., Eisel, U.L., Manahan-Vaughan, D., Jansen, S., Lienenklaus, S., Lu, B., Imai, Y., Muller, M., Goelz, S.E., Baker, D.P., Schwaninger, M., Kann, O., Heikenwalder, M., Kalinke, U., Prinz, M., 2016. Brain endothelial- and epithelial-specific interferon receptor chain 1 drives virus-induced sickness behavior and cognitive impairment. Immunity 44, 901–912.

Blasius, A.L., Giurisato, E., Cella, M., Schreiber, R.D., Shaw, A.S., Colonna, M., 2006. Bone marrow stromal cell antigen 2 is a specific marker of type I IFN-producing cells in the naive mouse, but a promiscuous cell surface antigen following IFN stimulation. J. Immunol. 177, 3260–3265.

Borna, R.M., Jahr, J.S., Kmiecik, S., Mancuso, K.F., Kaye, A.D., 2017. Pharmacology of octreotide: clinical implications for anesthesiologists and associated risks. Anesthesiol. Clin. 35, 327–339.

Brewitz, A., Eickhoff, S., Dahling, S., Quast, T., Bedoui, S., Kroczek, R.A., Kurts, C., Garbi, N., Barchet, W., Iannacone, M., Klauschen, F., Kolanus, W., Kaisho, T., Colonna, M., Germain, R.N., Kastenmuller, W., 2017. CD8(+) T cells orchestrate pDC-XCR1(+) dendritic cell spatial and functional cooperativity to optimize priming. Immunity 46, 205–219.

Brod, S.A., Hood, Z.M., 2011. Ingested (oral) SST inhibits EAE. Autoimmunity 44, 437–443.

Brown, K.N., Wijewardana, V., Liu, X., Barratt-Boyes, S.M., 2009. Rapid influx and death of plasmacytoid dendritic cells in lymph nodes mediate depletion in acute simian immunodeficiency virus infection. PLoS Pathog. 5, e1000413.

Budd, A., Alleva, L., Alsharifi, M., Koskinen, A., Smythe, V., Mullbacher, A., Wood, J., Clark, I., 2007. Increased survival after gemfibrozil treatment of severe mouse influenza. Antimicrob. Agents Chemother. 51, 2965–2968.

Burgus, R., Ling, N., Butcher, M., Guillemin, R., 1973. Primary structure of somatostatin, a hypothalamic peptide that inhibits the secretion of pituitary growth hormone. PNAS 70, 684–688.

Capuron, L., Gumnick, J.F., Musselman, D.L., Lawson, D.H., Reemsnyder, A., Nemeroff, C.B., Miller, A.H., 2002. Neurobehavioral effects of interferon-alpha in cancer patients: phenomenology and paroxetine responsiveness of symptom dimensions. Neuropsychopharmacology 26, 643–652.

Capuron, L., Miller, A.H., 2004. Cytokines and psychopathology: lessons from interferon-alpha. Biol. Psychiatry 56, 819–824.

Caraux, A., Kim, N., Bell, S.E., Zompi, S., Ranson, T., Lesjean-Pottier, S., Garcia-Ojeda, M. E., Turner, M., Colucci, F., 2006. Phospholipase C-gamma2 is essential for NK cell cytotoxicity and innate immunity to malignant and virally infected cells. Blood 107, 994–1002.

Chiba, T., Taminato, T., Kadowaki, S., Abe, H., Chihara, K., Seino, Y., Matsukura, S., Fujita, T., 1980. Effects of glucagon, secretin, and vasoactive intestinal polypeptide on gastric somatostatin and gastrin release from isolated perfused rat stomach. YGAST 79, 67–71.

Considine, R.V., Sinha, M.K., Heiman, M.L., Kriauciunas, A., Stephens, T.W., Nyce, M.R., Ohannesian, J.P., Marco, C.C., McKee, L.J., Bauer, T.L., et al., 1996. Serum immunoreactive-leptin concentrations in normal-weight and obese humans. N. Engl. J. Med. 334, 292–295.

Cowley, M.A., Smith, R.G., Diano, S., Tschop, M., Pronchuk, N., Grove, K.L., Strasburger, C.J., Bidlingmaier, M., Esterman, M., Heiman, M.L., Garcia-Segura, L.

M., Nillni, E.A., Mendez, P., Low, M.J., Sotonyi, P., Friedman, J.M., Liu, H., Pinto, S., Colmers, W.F., Cone, R.D., Horvath, T.L., 2003. The distribution and mechanism of action of ghrelin in the CNS demonstrates a novel hypothalamic circuit regulating energy homeostasis. Neuron 37, 649–661.

Crouse, J., Kalinke, U., Oxenius, A., 2015. Regulation of antiviral T cell responses by type I interferons. Nat. Rev. Immunol. 15, 231–242.

Dai, P., Wang, W., Cao, H., Avogadri, F., Dai, L., Drexler, I., Joyce, J.A., Li, X.D., Chen, Z., Merghoub, T., Shuman, S., Deng, L., 2014. Modified vaccinia virus Ankara triggers type I IFN production in murine conventional dendritic cells via a cGAS/STING-mediated cytosolic DNA-sensing pathway. PLoS Pathog. 10, e1003989.

Dantzer, R., 2001. Cytokine-induced sickness behavior: mechanisms and implications. Ann. N. Y. Acad. Sci. 933, 222–234.

DiGruccio, M.R., Mawla, A.M., Donaldson, C.J., Noguchi, G.M., Vaughan, J., Cowing-Zitron, C., van der Meulen, T., Huising, M.O., 2016. Comprehensive alpha, beta and delta cell transcriptomes reveal that ghrelin selectively activates delta cells and promotes somatostatin release from pancreatic islets. Mol. Metab. 5, 449–458.

Dixit, V.D., Schaffer, E.M., Pyle, R.S., Collins, G.D., Sakthivel, S.K., Palaniappan, R., Lillard Jr., J.W., Taub, D.D., 2004. Ghrelin inhibits leptin- and activation-induced proinflammatory cytokine expression by human monocytes and T cells. J. Clin. Investig. 114, 57–66.

Eissele, R., Koop, H., Arnold, R., 1990. Effect of glucagon-like peptide-1 on gastric somatostatin and gastrin secretion in the rat. Scand. J. Gastroenterol. 25, 449–454.

Falnes, P.O., Ariansen, S., Sandvig, K., Olsnes, S., 2000. Requirement for prolonged action in the cytosol for optimal protein synthesis inhibition by diphtheria toxin. J. Biol. Chem. 275, 4363–4368.

Farsakoglu, Y., Palomino-Segura, M., Latino, I., Zanaga, S., Chatziandreou, N., Pizzagalli, D.U., Rinaldi, A., Bolis, M., Sallusto, F., Stein, J.V., Gonzalez, S.F., 2019. Influenza vaccination induces NK-cell-mediated Type-II IFN response that regulates humoral immunity in an IL-6-dependent manner. Cell. Rep. 26 (2307–2315), e2305.

Flogstad, A.K., Halse, J., Bakke, S., Lancranjan, I., Marbach, P., Bruns, C., Jervell, J., 1997. Sandostatin LAR in acromegalic patients: long-term treatment. J. Clin. Endocrinol. Metab. 82, 23–28.

Gill, S., Vasey, A.E., De Souza, A., Baker, J., Smith, A.T., Kohrt, H.E., Florek, M., Gibbs Jr., K.D., Tate, K., Ritchie, D.S., Negrin, R.S., 2012. Rapid development of exhaustion and down-regulation of eomesodermin limit the antitumor activity of adoptively transferred murine natural killer cells. Blood 119, 5758–5768.

Gilliet, M., Cao, W., Liu, Y.J., 2008. Plasmacytoid dendritic cells: sensing nucleic acids in viral infection and autoimmune diseases. Nat. Rev. Immunol. 8, 594–606.

Goto, Y., Berelowitz, M., Frohman, L.A., 1981. Effect of catecholamines on somatostatin secretion by isolated perfused rat stomach. Am. J. Physiol. 240, E274–278.

Han, M.S., White, A., Perry, R.J., Camporez, J.P., Hidalgo, J., Shulman, G.I., Davis, R.J., 2020. Regulation of adipose tissue inflammation by interleukin 6. Proc. Natl. Acad. Sci. USA 117, 2751–2760.

Hart, B.L., 1988. Biological basis of the behavior of sick animals. Neurosci. Biobehav. Rev. 12, 123–137.

Hart, B.L., Hart, L.A., 2018. How mammals stay healthy in nature: the evolution of behaviours to avoid parasites and pathogens. Philos. Trans. R. Soc. Lond. B Biol. Sci. 373.

Hauge-Evans, A.C., Bowe, J., Franklin, Z.J., Hassan, Z., Jones, P.M., 2015. Inhibitory effect of somatostatin on insulin secretion is not mediated via the CNS. J. Endocrinol. 225, 19–26.

Hauge-Evans, A.C., King, A.J., Carmignac, D., Richardson, C.C., Robinson, I.C., Low, M. J., Christie, M.R., Persaud, S.J., Jones, P.M., 2009. Somatostatin secreted by islet delta-cells fulfills multiple roles as a paracrine regulator of islet function. Diabetes 58, 403–411.

Henson, S.M., Franzese, O., Macaulay, R., Libri, V., Azevedo, R.I., Kiani-Alikhan, S., Plunkett, F.J., Masters, J.E., Jackson, S., Griffiths, S.J., Pircher, H.P., Soares, M.V., Akbar, A.N., 2009. KLRG1 signaling induces defective Akt (ser473) phosphorylation and proliferative dysfunction of highly differentiated CD8+ T cells. Blood 113, 6619–6628.

Honda, K., Ohba, Y., Yanai, H., Negishi, H., Mizutani, T., Takaoka, A., Taya, C., Taniguchi, T., 2005. Spatiotemporal regulation of MyD88-IRF-7 signalling for robust type-I interferon induction. Nature 434, 1035–1040.

Howick, K., Griffin, B.T., Cryan, J.F., Schellekens, H., 2017. From belly to brain: targeting the ghrelin receptor in appetite and food intake regulation. Int. J. Mol. Sci. 18.

Isaacs, A., Lindenmann, J., 1957. Virus interference. I. The interferon. Proc. Royal Soc. London Ser. B, Biol. Sci. 147, 258–267.

Isaacs, A., Lindenmann, J., Valentine, R.C., 1957. Virus interference. II. Some properties of interferon. Proc. Royal Soc. London Ser. B Biol. Sci. 147, 268–273.

Jiang, K., Zhong, B., Gilvary, D.L., Corliss, B.C., Hong-Geller, E., Wei, S., Djeu, J.Y., 2000. Pivotal role of phosphoinositide-3 kinase in regulation of cytotoxicity in natural killer cells. Nat. Immunol. 1, 419–425.

Kawai, T., Akira, S., 2011. Toll-like receptors and their crosstalk with other innate receptors in infection and immunity. Immunity 34, 637–650.

Kelley, K.W., Bluthe, R.M., Dantzer, R., Zhou, J.H., Shen, W.H., Johnson, R.W., Broussard, S.R., 2003. Cytokine-induced sickness behavior. Brain Behav. Immun. 17 (Suppl 1), S112–118.

Kent, S., Bret-Dibat, J.L., Kelley, K.W., Dantzer, R., 1996. Mechanisms of sickness-induced decreases in food-motivated behavior. Neurosci. Biobehav. Rev. 20, 171–175.

Kolumam, G.A., Thomas, S., Thompson, L.J., Sprent, J., Murali-Krishna, K., 2005. Type I interferons act directly on CD8 T cells to allow clonal expansion and memory formation in response to viral infection. J. Exp. Med. 202, 637–650.

Langhans, W., Hrupka, B., 1999. Interleukins and tumor necrosis factor as inhibitors of food intake. Neuropeptides 33, 415–424.

Leuschen, M.P., Filipi, M., Healey, K., 2004. A randomized open label study of pain medications (naproxen, acetaminophen and ibuprofen) for controlling side effects during initiation of IFN beta-1a therapy and during its ongoing use for relapsing-remitting multiple sclerosis. Mult. Scler. 10, 636–642.

Luque, R.M., Gahete, M.D., Hochgeschwender, U., Kineman, R.D., 2006. Evidence that endogenous SST inhibits ACTH and ghrelin expression by independent pathways. Am. J. Physiol. Endocrinol. Metab. 291, E395–403.

Lustig, R.H., Hinds, P.S., Ringwald-Smith, K., Christensen, R.K., Kaste, S.C., Schreiber, R. E., Rai, S.N., Lensing, S.Y., Wu, S., Xiong, X., 2003. Octreotide therapy of pediatric hypothalamic obesity: a double-blind, placebo-controlled trial. J. Clin. Endocrinol. Metab. 88, 2586–2592.

Machida, M., Ambrozewicz, M.A., Breving, K., Wellman, L.L., Yang, L., Ciavarra, R.P., Sanford, L.D., 2014. Sleep and behavior during vesicular stomatitis virus induced encephalitis in BALB/cJ and C57BL/6J mice. Brain Behav. Immun. 35, 125–134.

Maeda, T., Murata, K., Fukushima, T., Sugahara, K., Tsuruda, K., Anami, M., Onimaru, Y., Tsukasaki, K., Tomonaga, M., Moriuchi, R., Hasegawa, H., Yamada, Y., Kamihira, S., 2005. A novel plasmacytoid dendritic cell line, CAL-1, established from a patient with blastic natural killer cell lymphoma. Int. J. Hematol. 81, 148–154.

Marie, I., Smith, E., Prakash, A., Levy, D.E., 2000. Phosphorylation-induced dimerization of interferon regulatory factor 7 unmasks DNA binding and a bipartite transactivation domain. Mol. Cell. Biol. 20, 8803–8814.

Martin-Fontecha, A., Thomsen, L.L., Brett, S., Gerard, C., Lipp, M., Lanzavecchia, A., Sallusto, F., 2004. Induced recruitment of NK cells to lymph nodes provides IFN-gamma for T(H)1 priming. Nat. Immunol. 5, 1260–1265.

Matthys, P., Heremans, H., Opdenakker, G., Billiau, A., 1991. Anti-interferon-gamma antibody treatment, growth of Lewis lung tumours in mice and tumour-associated cachexia. Eur. J. Cancer 27, 182–187.

Matucci-Cerinic, M., Borrelli, F., Generini, S., Cantelmo, A., Marcucci, I., Martelli, F., Romagnoli, P., Bacci, S., Conz, A., Marinelli, P., et al., 1995. Somatostatin-induced modulation of inflammation in experimental arthritis. Arthritis Rheum. 38, 1687–1693.

McNab, F., Mayer-Barber, K., Sher, A., Wack, A., O'Garra, A., 2015. Type I interferons in infectious disease. Nat. Rev. Immunol. 15, 87–103.

Medina, E.A., Stanhope, K.L., Mizuno, T.M., Mobbs, C.V., Gregoire, F., Hubbard, N.E., Erickson, K.L., Havel, P.J., 1999. Effects of tumor necrosis factor alpha on leptin secretion and gene expression: relationship to changes of glucose metabolism in isolated rat adipocytes. Int. J. Obes. Relat. Metab. Disord. 23, 896–903.

Mishra, D., Richard, J.E., Maric, I., Porteiro, B., Haring, M., Kooijman, S., Musovic, S., Eerola, K., Lopez-Ferreras, L., Peris, E., Grycel, K., Shevchouk, O.T., Micallef, P., Olofsson, C.S., Wernstedt Asterholm, I., Grill, H.J., Nogueiras, R., Skibicka, K.P., 2019. Parabrachial interleukin-6 reduces body weight and food intake and increases thermogenesis to regulate energy metabolism. Cell Rep 26 (3011–3026), e3015.

Mrosovsky, N., Molony, L.A., Conn, C.A., Kluger, M.J., 1989. Anorexic effects of interleukin 1 in the rat. Am. J. Physiol. 257, R1315–1321.

Muller-Durovic, B., Lanna, A., Covre, L.P., Mills, R.S., Henson, S.M., Akbar, A.N., 2016. Killer cell lectin-like receptor G1 inhibits NK cell function through activation of adenosine 5'-monophosphate-activated protein kinase. J. Immunol. 197, 2891–2899.

Murray, M.J., Murray, A.B., 1979. Anorexia of infection as a mechanism of host defense. Am. J. Clin. Nutr. 32, 593–596.

Nakazato, M., Murakami, N., Date, Y., Kojima, M., Matsuo, H., Kangawa, K., Matsukura, S., 2001. A role for ghrelin in the central regulation of feeding. Nature 409, 194–198.

Narayanan, S., Surendranath, K., Bora, N., Surolia, A., Karande, A.A., 2005. Ribosome inactivating proteins and apoptosis. FEBS Lett. 579, 1324–1331.

Pascual, V., Chaussabel, D., Banchereau, J., 2010. A genomic approach to human autoimmune diseases. Annu. Rev. Immunol. 28, 535–571.

Porter, M.H., Arnold, M., Langhans, W., 1998. TNF-alpha tolerance blocks LPS-induced hypophagia but LPS tolerance fails to prevent TNF-alpha-induced hypophagia. Am. J. Physiol. 274, R741–745.

Reading, P.C., Whitney, P.G., Barr, D.P., Smyth, M.J., Brooks, A.G., 2006. NK cells contribute to the early clearance of HSV-1 from the lung but cannot control replication in the central nervous system following intranasal infection. Eur. J. Immunol. 36, 897–905.

Riechelmann, R.P., Pereira, A.A., Rego, J.F., Costa, F.P., 2017. Refractory carcinoid syndrome: a review of treatment options. Ther. Adv. Med. Oncol. 9, 127–137.

Rorsman, P., Huising, M.O., 2018. The somatostatin-secreting pancreatic delta-cell in health and disease. Nat. Rev. Endocrinol. 14, 404–414.

Saito, M., Iwawaki, T., Taya, C., Yonekawa, H., Noda, M., Inui, Y., Mekada, E., Kimata, Y., Tsuru, A., Kohno, K., 2001. Diphtheria toxin receptor–mediated conditional and targeted cell ablation in transgenic mice. Nat. Biotechnol. 19, 746–750.

Schlitzer, A., Sivakamasundari, V., Chen, J., Sumatoh, H.R.B., Schreuder, J., Lum, J., Malleret, B., Zhang, S., Larbi, A., Zolezzi, F., Renia, L., Poidinger, M., Naik, S., Newell, E.W., Robson, P., Ginhoux, F., 2015. Identification of cDC1- and cDC2-committed DC progenitors reveals early lineage priming at the common DC progenitor stage in the bone marrow. Nat. Immunol. 16, 718–728.

Shimada, M., Date, Y., Mondal, M.S., Toshinai, K., Shimbara, T., Fukunaga, K., Murakami, N., Miyazato, M., Kangawa, K., Yoshimatsu, H., Matsuo, H., Nakazato, M., 2003. Somatostatin suppresses ghrelin secretion from the rat stomach. Biochem. Biophys. Res. Commun. 302, 520–525.

Strauss, N., 1960. The effect of diphtheria toxin on the metabolism of hela cells: II. Effect on nucleic acid metabolism. J. Exp. Med. 112, 351–359.

Strauss, N., Hendee, E.D., 1959. The effect of diphtheria toxin on the metabolism of HeLa cells. J. Exp. Med. 109, 145–163.

Strickertsson, J.A.B., Døssing, K.B.V., Aabakke, A.J.M., Nilsson, H.-O., Hansen, T.V.O., Knigge, U., Kjær, A., Wadström, T., Friis-Hansen, L., 2011. Interferon-γ inhibits ghrelin expression and secretion via a somatostatin-mediated mechanism. World J. Gastroenterol. 17, 3117–3125.

Strowski, M.Z., Parmar, R.M., Blake, A.D., Schaeffer, J.M., 2000. Somatostatin inhibits insulin and glucagon secretion via two receptors subtypes: an in vitro study of pancreatic islets from somatostatin receptor 2 knockout mice. Endocrinology 141, 111–117.

Swiecki, M., Gilfillan, S., Vermi, W., Wang, Y., Colonna, M., 2010. Plasmacytoid dendritic cell ablation impacts early interferon responses and antiviral NK and CD8(+) T cell accrual. Immunity 33, 955–966.

Swiecki, M., Wang, Y., Vermi, W., Gilfillan, S., Schreiber, R.D., Colonna, M., 2011. Type I interferon negatively controls plasmacytoid dendritic cell numbers in vivo. J. Exp. Med. 208, 2367–2374.

Tang-Christensen, M., Vrang, N., Ortmann, S., Bidlingmaier, M., Horvath, T.L., Tschöp, M., 2004. Central administration of ghrelin and agouti-related protein (83–132) increases food intake and decreases spontaneous locomotor activity in rats. Endocrinology 145, 4645–4652.

Timper, K., Denson, J.L., Steculorum, S.M., Heilinger, C., Engstrom-Ruud, L., Wunderlich, C.M., Rose-John, S., Wunderlich, F.T., Bruning, J.C., 2017. IL-6 improves energy and glucose homeostasis in obesity via enhanced central IL-6 trans-signaling. Cell. Rep. 19, 267–280.

Tomasello, E., Naciri, K., Chelbi, R., Bessou, G., Fries, A., Gressier, E., Abbas, A., Pollet, E., Pierre, P., Lawrence, T., Vu Manh, T.P., Dalod, M., 2018. Molecular dissection of plasmacytoid dendritic cell activation in vivo during a viral infection. EMBO J. 37.

Tomasello, E., Pollet, E., Vu Manh, T.P., Uze, G., Dalod, M., 2014. Harnessing mechanistic knowledge on beneficial versus deleterious IFN-I effects to design innovative immunotherapies targeting cytokine activity to specific cell types. Front. Immunol. 5, 526.

Tschop, M., Smiley, D.L., Heiman, M.L., 2000. Ghrelin induces adiposity in rodents. Nature 407, 908–913.

Turrin, N.P., Ilyin, S.E., Gayle, D.A., Plata-Salaman, C.R., Ramos, E.J., Laviano, A., Das, U.N., Inui, A., Meguid, M.M., 2004. Interleukin-1beta system in anorectic catabolic tumor-bearing rats. Curr. Opin. Clin. Nutr. Metab. Care 7, 419–426.

Tzotzas, T., Papazisis, K., Perros, P., Krassas, G.E., 2008. Use of somatostatin analogues in obesity. Drugs 68, 1963–1973.

Waibler, Z., Anzaghe, M., Ludwig, H., Akira, S., Weiss, S., Sutter, G., Kalinke, U., 2007. Modified vaccinia virus Ankara induces Toll-like receptor-independent type I interferon responses. J. Virol. 81, 12102–12110.

Wallenius, K., Wallenius, V., Sunter, D., Dickson, S.L., Jansson, J.O., 2002. Intracerebroventricular interleukin-6 treatment decreases body fat in rats. Biochem. Biophys. Res. Commun. 293, 560–565.

Wang, A., Huen, S.C., Luan, H.H., Yu, S., Zhang, C., Gallezot, J.D., Booth, C.J., Medzhitov, R., 2016. Opposing effects of fasting metabolism on tissue tolerance in bacterial and viral inflammation. Cell 166 (1512–1525), e1512.

Wang, B.X., Fish, E.N., 2012. The yin and yang of viruses and interferons. Trends Immunol. 33, 190–197.

Wang, J.M., Cheng, Y.Q., Shi, L., Ying, R.S., Wu, X.Y., Li, G.Y., Moorman, J.P., Yao, Z.Q., 2013. KLRG1 negatively regulates natural killer cell functions through the Akt pathway in individuals with chronic hepatitis C virus infection. J. Virol. 87, 11626–11636.

Wasada, T., Howard, B., Dobbs, R.E., Unger, R.H., 1980. Evidence for a role of free fatty acids in the regulation of somatostatin secretion in normal and alloxan diabetic dogs. J. Clin. Investig. 66, 511–516.

Whitmire, J.K., Tan, J.T., Whitton, J.L., 2005. Interferon-gamma acts directly on CD8+ T cells to increase their abundance during virus infection. J. Exp. Med. 201, 1053–1059.

Wing, E.J., Young, J.B., 1980. Acute starvation protects mice against Listeria monocytogenes. Infect. Immun. 28, 771–776.

Wren, A.M., Small, C.J., Ward, H.L., Murphy, K.G., Dakin, C.L., Taheri, S., Kennedy, A.R., Roberts, G.H., Morgan, D.G., Ghatei, M.A., Bloom, S.R., 2000. The novel hypothalamic peptide ghrelin stimulates food intake and growth hormone secretion. Endocrinology 141, 4325–4328.

Wueest, S., Konrad, D., 2018. The role of adipocyte-specific IL-6-type cytokine signaling in FFA and leptin release. Adipocyte 7, 226–228.

Yamazaki, C., Sugiyama, M., Ohta, T., Hemmi, H., Hamada, E., Sasaki, I., Fukuda, Y., Yano, T., Nobuoka, M., Hirashima, T., Iizuka, A., Sato, K., Tanaka, T., Hoshino, K., Kaisho, T., 2013. Critical roles of a dendritic cell subset expressing a chemokine receptor, XCR1. J. Immunol. 190, 6071–6082.

Yang, L.P., Keating, G.M., 2010. Octreotide long-acting release (LAR): a review of its use in the management of acromegaly. Drugs 70, 1745–1769.

Zigman, J.M., Jones, J.E., Lee, C.E., Saper, C.B., Elmquist, J.K., 2006. Expression of ghrelin receptor mRNA in the rat and the mouse brain. J. Comp. Neurol. 494, 528–548.